THE PLANT CELL

FRUITFULL-like genes regulate flowering time and inflorescence architecture in tomato

Research Article

Xiaobing Jiang [iD] ,[1,2] Greice Lubini [iD] ,[2,3,4] José Hernandes-Lopes [iD] ,[2,5] Kim Rijnsburger [iD] ,[1] Vera Veltkamp [iD] ,[1,2] Ruud A. de Maagd [iD] ,[2] Gerco C. Angenent [iD] [1,2] and Marian Bemer [iD] [1,2,*,†]

1   Laboratory of Molecular Biology, Wageningen University and Research, Droevendaalsesteeg 1, 6708 PB Wageningen, The Netherlands
2   Business Unit Bioscience, Wageningen University and Research, Droevendaalsesteeg 1, 6708 PB Wageningen, The Netherlands
3   Departamento de Biologia, Faculdade de Filosofia, Ciências e Letras de Ribeirão Preto, Universidade de São Paulo, Ribeirão Preto 14040-901, Brazil
4   PPG-Genética, Faculdade de Medicina de Ribeirão Preto, Universidade de São Paulo, Ribeirão Preto 14049-900, Brazil
5   Departamento de Botânica, Instituto de Biociências, Universidade de São Paulo, Rua do Matão 277, 05508-090 São Paulo, Brazil

*Author for correspondence: marian.bemer@wur.nl
†Senior author.

M.B. conceived the project and designed the experiments. X.J. performed the qPCRs, tomato CRISPR/cas9 mutagenesis, RNA-seq experiments, EMSAs, SEM analysis, and CK reporter identification. K.R., G.L., and J.H.-L. did the Y2H analyses. V.V. measured the fruit phenotypes. R.A.d.M. analyzed *FUL1* alleles in cultivars and assisted with the RNA-seq analysis. G.C.A. and M.B. supervised the project. M.B. and X.J. analyzed the data, prepared the figures, and wrote the article. All authors read and approved the final version.

The author responsible for distribution of materials integral to the findings presented in this article in accordance with the policy described in the Instructions for Authors (https://academic.oup.com/plcell) is: Marian Bemer (marian.bemer@wur.nl).

Abstract

The timing of flowering and the inflorescence architecture are critical for the reproductive success of tomato (*Solanum lycopersicum*), but the gene regulatory networks underlying these traits have not been fully explored. Here, we show that the tomato *FRUITFULL*-like (*FUL*-like) genes *FUL2* and *MADS-BOX PROTEIN 20* (*MBP20*) promote the vegetative-to-reproductive transition and repress inflorescence branching by inducing floral meristem (FM) maturation. *FUL1* fulfils a less prominent role and appears to depend on FUL2 and MBP20 for its upregulation in the inflorescence- and floral meristems. *MBP10*, the fourth tomato *FUL*-like gene, has probably lost its function. The tomato FUL-like proteins cannot homodimerize in in vitro assays, but heterodimerize with various other MADS-domain proteins, potentially forming distinct complexes in the transition meristem and FM. Transcriptome analysis of the primary shoot meristems revealed various interesting downstream targets, including four repressors of cytokinin signaling that are upregulated during the floral transition in *ful1 ful2 mbp10 mbp20* mutants. FUL2 and MBP20 can also bind in vitro to the upstream regions of these genes, thereby probably directly stimulating cell division in the meristem upon the transition to flowering. The control of inflorescence branching does not occur via the cytokinin oxidase/dehydrogenases (CKXs) but may be regulated by repression of transcription factors such as *TOMATO MADS-box gene 3* (*TM3*) and *APETALA 2b* (*AP2b*).

Introduction

The MADS-box transcription factor gene family is involved in almost every developmental process in plants (Smaczniak et al., 2012a), and the members of the angiosperm-specific *APETALA1/FRUITFULL* (*AP1/FUL*) subfamily play key roles in flowering and fruit development (Litt and Irish, 2003; McCarthy et al., 2015). In the core eudicots, the *AP1/FUL*

Open Access

subfamily consists of three clades, *euAP1*, *euFULI*, and *euFULII* (Litt and Irish, 2003). The *Arabidopsis thaliana* genome carries four *AP1/FUL*-clade genes, with *AP1* functioning as a key regulator of floral initiation and floral meristem (FM) establishment, and acting as an A-class gene in the ABC model (Ferrándiz et al., 2000; Kaufmann et al., 2010), promoting perianth identity (Mandel et al., 1992; Theissen and Saedler, 2001). Its lower expressed paralog *CAULIFLOWER* (*CAL*) functions to a large extent redundantly with *AP1* (Bowman et al., 1993; Ye et al., 2016). The *euFULII*-clade gene *AGAMOUS-LIKE 79* (*AGL79*) appears to have a minor function in roots (Gao et al., 2018), whereas the *euFULI* gene *FUL* is a pleiotropic gene. In addition to its key role in fruit development (Gu et al., 1998), *FUL* regulates many aspects of flowering in Arabidopsis, including flowering time (Ferrándiz et al., 2000; Melzer et al., 2008), repression of inflorescence meristem (IM) identity (together with *AP1/CAL*; Ferrándiz et al., 2000), inflorescence architecture (Bemer et al., 2017), axillary inflorescence outgrowth (together with *SUPPRESSOR OF OVEREXPRESSION OF CONSTANS1* (*SOC1*) (Karami et al., 2020)) and IM termination (Balanzà et al., 2018). In a wide range of angiosperm species, *FUL*-like genes regulate flowering (Ferrándiz et al., 2000; Berbel et al., 2012; Pabón-Mora et al., 2012, 2013; Ping et al., 2014; Jia et al., 2015; Jaudal et al., 2015; Li et al., 2019; Zhang et al., 2021) and fruit development (Gu et al., 1998; Jaakola et al., 2010; Bemer et al., 2012; Pabón-Mora et al., 2012, 2013; Zhao et al., 2019). In tomato (*Solanum lycopersicum*), the *euFULI*-clade genes *S. lycopersicum FUL1* (*SlFUL1/TM4/TDR4*, hereafter called *FUL1*) and *SlFUL2* (*FUL2/MBP7*, hereafter called *FUL2*) play important roles in fruit development and ripening (Bemer et al., 2012; Shima et al., 2013; Wang et al., 2019), but flowering phenotypes have not yet been described for these genes, nor for the tomato *euFULII*-clade genes *MADS-BOX PROTEIN 10* (*MBP10*) and *MBP20*. This is remarkable given the strong upregulation of *FUL1*, *FUL2*, and *MBP20* expression during the transition from shoot apical meristem (SAM) to FM/IM (Park et al., 2012).

Flowering is an important agricultural trait in tomato, because the onset and termination of flowering, as well as the inflorescence architecture, determine crop yield. Tomato is also an interesting model species considering its sympodial shoot architecture, which is distinct from that of the monopodial Arabidopsis. While the Arabidopsis SAM develops into an IM, which subsequently forms FMs on its flank (indeterminate inflorescence), the tomato SAM domes to form the transition meristem (TM) that terminates directly into an FM (determinate inflorescence), but forms a new IM on its flank. This iterative process results in a zigzagged inflorescence (Lippman et al., 2008). Moreover, tomato has a compound shoot, which resumes vegetative growth from the axillary meristem of the youngest leaf axil when the inflorescence has formed. After activation of the axillary meristem (then called sympodial meristem, SYM), the shoot forms three leaves before terminating again into the first flower of the second inflorescence (Pnueli et al., 1998; Szymkowiak and Irish, 2006; Lippman et al., 2008), upon which a new axillary meristem takes over vegetative growth. This process forms the compound shoot, where three leaves and an inflorescence comprise a sympodial unit, a pattern that is endlessly repeated in the wild-type (WT) tomato.

The genes that regulate these flowering processes have been very well studied in the indeterminate Arabidopsis inflorescence, where the floral integrators FLOWERING LOCUS T (FT) and SOC1 regulate the transition to flowering, after which TERMINAL FLOWER 1 (TFL1) determines IM fate by repressing FM genes such as *LEAFY* (*LFY*) and *AP1* (Sablowski, 2007; Lee and Lee, 2010; Serrano-Mislata et al., 2017; Zhu et al., 2020), while AP1 on its turn represses *TFL1*, so that clear borders between the FM and IM are achieved (Liu et al., 2013; Goslin et al., 2017). The variation in inflorescence structures of different species can be largely explained by different temporal and spatial expression of flower-repressing *TFL1* homologs and flower-inducing *LFY/AP1/FUL* homologs on the other side (McGarry and Ayre, 2012; Périlleux et al., 2019). In legumes, for example, the indeterminate inflorescence does not form FMs on its flank, but secondary IMs, due to repression of the *TFL1*-homolog in these meristems by the euFULII clade proteins VEG1 (pea, *Pisum sativum*) or MtFUL1-c (Medicago, *Medicago truncatula*) (Berbel et al., 2012; Cheng et al., 2018; Zhang et al., 2021). These secondary IMs do form FMs, resulting in a compound inflorescence (Benlloch et al., 2015).

In tomato, SINGLE FLOWER TRUSS (*SFT*, homolog of *FT*), FALSIFLORA (*FA*, homolog of *LFY*), and MACROCALYX (*MC*, homolog of *AP1*) are essential for the transition to flowering and control of FM identity similar to their orthologs in Arabidopsis (Molinero-Rosales et al., 1999; Molinero-Rosales et al., 2004; Yuste-Lisbona et al., 2016). However, mutants in the *TFL1*-ortholog *SELF-PRUNING* (*SP*), which is not expressed in the primary vegetative SAM (VM), but highly expressed in axillary meristems (Thouet et al., 2008), lose this growth indeterminacy and terminate their SYMs early, resulting in the termination of growth after a few sympodial units (Pnueli et al., 1998). Inflorescence architecture is normal in an *sp* mutant (Pnueli et al., 1998). Instead, tomato inflorescence architecture is influenced by other factors that regulate the timing of FM maturation (Lippman et al., 2008). Failure of meristem maturation in the *fa* and *anantha* (*an*, homolog of *UFO*) mutants, or largely delayed maturation in *compound inflorescences* (*s*, homolog of *WOX9*) mutant induce additional IM formations, resulting in highly branched (compound) inflorescences (Szymkowiak and Irish, 2006; Chae et al., 2008; Lippman et al., 2008; Souer et al., 2008; Park et al., 2012; Soyk et al., 2017). Conversely, precocious activation of the AN/FA complex leads to early FM maturation and thus early flowering (MacAlister et al., 2012). In addition to these factors, several MADS-domain transcription factors function in tomato flowering, mainly in conferring IM or FM identity. In the *jointless* (*j*, homolog of *SVP*) and *mc* mutants, flowering is delayed and the inflorescence reverts to vegetative growth after a few flowers,

probably because the FM flanking meristems adopt VM/SYM identity instead of IM fate (Szymkowiak and Irish, 2006; Yuste-Lisbona et al., 2016). Mutations in the *SEPALLATA* (*SEP*)-like genes *JOINTLESS 2* (*J2/SlMBP21*), *ENHANCER OF JOINTLESS 2* (*EJ2/MADS1*) and the *SOC1*-like genes *TM3* and *SISTER OF TM3* (*STM3*) affect inflorescence branching through yet uncharacterized mechanisms (Roldan et al., 2017; Soyk et al., 2017, 2019; Alonge et al., 2020). Interestingly, the *tm3 stm3* mutations suppress the enhanced branching phenotype of the *j2 ej2* mutant (Alonge et al., 2020), suggesting that these MADS-domain transcription factors have an opposite function in FM development. Natural mutations or structural variants in several of these MADS-box genes have been important for domestication, either through the regulation of flower/fruit abscission (*MC*, *J*, *J2*) or inflorescence architecture (*J2*, *EJ2*, *TM3*, *STM3*) (Nakano et al., 2012; Liu et al., 2014; Soyk et al., 2019; Alonge et al., 2020). Thus, although tomato inflorescence development differs fundamentally from that of monopodial species such as Arabidopsis, the orthologs of several important Arabidopsis flowering and IM genes are also essential in tomato. However, it is yet unclear if and how the *FUL*-like genes (*SlFULs*) function in the tomato flowering regulatory network.

Here, we investigated the developmental roles of the four *SlFULs* in tomato by CRISPR/Cas9-mutagenesis and transcriptome profiling. We demonstrate that subfunctionalization has occurred after duplication within the Solanaceae *euFULI* and *euFULII* clades, and that the *FUL1* sequence has undergone further divergence during tomato domestication and breeding. *FUL2* and *MBP20* are highly expressed in the meristem during the vegetative-to-reproductive transition to additively promote tomato flowering and to repress inflorescence branching together with *FUL1*. Transcriptome analysis in the *ful1 ful2 mbp10 mbp20* quadruple mutant revealed that the *SlFULs* act probably parallel to, or downstream of, previously described key regulators such as *SFT*, *FA*, and *AN* during both the VM-to-TM transition and the establishment of inflorescence architecture. Furthermore, our target gene analysis revealed that the delay in transition to flowering may be explained by reduced cytokinin (CK) signaling as a result of upregulation of cytokinin oxidases/dehydrogenases (*CKXs*), while the increased branching is caused by delayed FM maturation as a possible result of specific MADS-domain and *AP2*-like transcription factors that are upregulated in the mutant.

Results

Expression patterns and protein–protein interaction profiles differ between the SlFULs

To investigate to what extent the SlFULs may have overlapping functions in specific organs, we performed expression profiling using reverse transcription quantitative polymerase chain reaction (RT-qPCR) in the cultivar Moneyberg (Figure 1, A). *FUL1* and *FUL2* were expressed very weakly during vegetative growth and had increased expression in the IM-enriched sample. Their expression remained high throughout reproductive development, where both genes showed considerable expression in all floral whorls and all stages of fruit development. *FUL2*, in particular, was strongly expressed in all floral organs, early fruits, and ripening fruits, while *FUL1* expression was moderate until the fruit ripening phase, when it increased strongly as reported previously (Bemer et al., 2012). Our data also revealed striking differences in spatial expression, with *MBP10* and *MBP20* expressed to much lower levels than *FUL1* and *FUL2* in the reproductive tissues, except for the expression of *MBP20* in the IM. *MBP10* especially was extremely weakly expressed, with detectable levels in stem and flower bud only.

MADS-domain transcription factors regulate multiple developmental processes by forming dimeric or higher order complexes (De Folter et al., 2005; Immink et al., 2009). To investigate which protein complexes may be formed by the different SlFUL proteins, we performed a yeast-two hybrid (Y2H) assay to identify the interactions of FUL1, FUL2, MBP10, and MBP20 with other tomato MADS-domain family proteins (Figure 1, B and Supplemental Figure S1). We chose a set of proteins homologous to MADS-domain proteins known to interact with Arabidopsis FUL (AtFUL) (De Folter et al., 2005). While AtFUL can form homodimers (Smaczniak et al., 2012b), none of the SlFUL proteins possessed this capacity, nor could they heterodimerize with each other (Supplemental Figure S1). Of the tested MADS-domain proteins, MC, SlMBP9, SlMBP12, SlMBP13, SlMBP14, SlMBP22, and SlMBP24 did not interact with any of the SlFUL proteins. Our screen showed that the SlFULs could interact with 10 other tomato MADS-domain proteins and we observed clear differences between the interaction profiles of FUL1, FUL2, MBP10, and MBP20. All SlFUL proteins interacted with J, J2, TM3, STM3 and the fruit-ripening regulator MADS-RIN. FUL2 exhibited the most extensive interaction network, interacting with all 10 proteins. It is the only protein that strongly interacted with the SEP-like proteins EJ2 and LeSEP1/TM29 (TM29-BD only with FUL2-AD, see Supplemental Figure S1), and with TAG1 (ortholog of AG) (Figure 1, B and Supplemental Figure S1). The latter interaction is especially interesting in the light of the high expression of *FUL2* in pistils, where FUL2 may have a specific function in a complex with the co-expressed TAG1. In addition to these specific interactions, FUL2, FUL1, and MBP20 share interactions with the SEP-like protein TM5 and with FOREVER YOUNG FLOWER-LIKE (FYFL/SlMBP18, homolog of AGL42), and FUL1 could also weakly interact with EJ2 (Supplemental Figure S1). Some of the interaction pairs we tested have been investigated before in a tomato MADS-domain interaction screen (Leseberg et al., 2008). We could reproduce all the previous results, except for interactions of FUL2 and MBP20 with SlMBP13, and FUL2 with SlMBP24. In conclusion, FUL2 can form most protein–protein interactions, which, together with its broad expression pattern, suggests that it can fulfil multiple functions in tomato, similar to AtFUL. FUL1 and MBP20 share a reduced set of
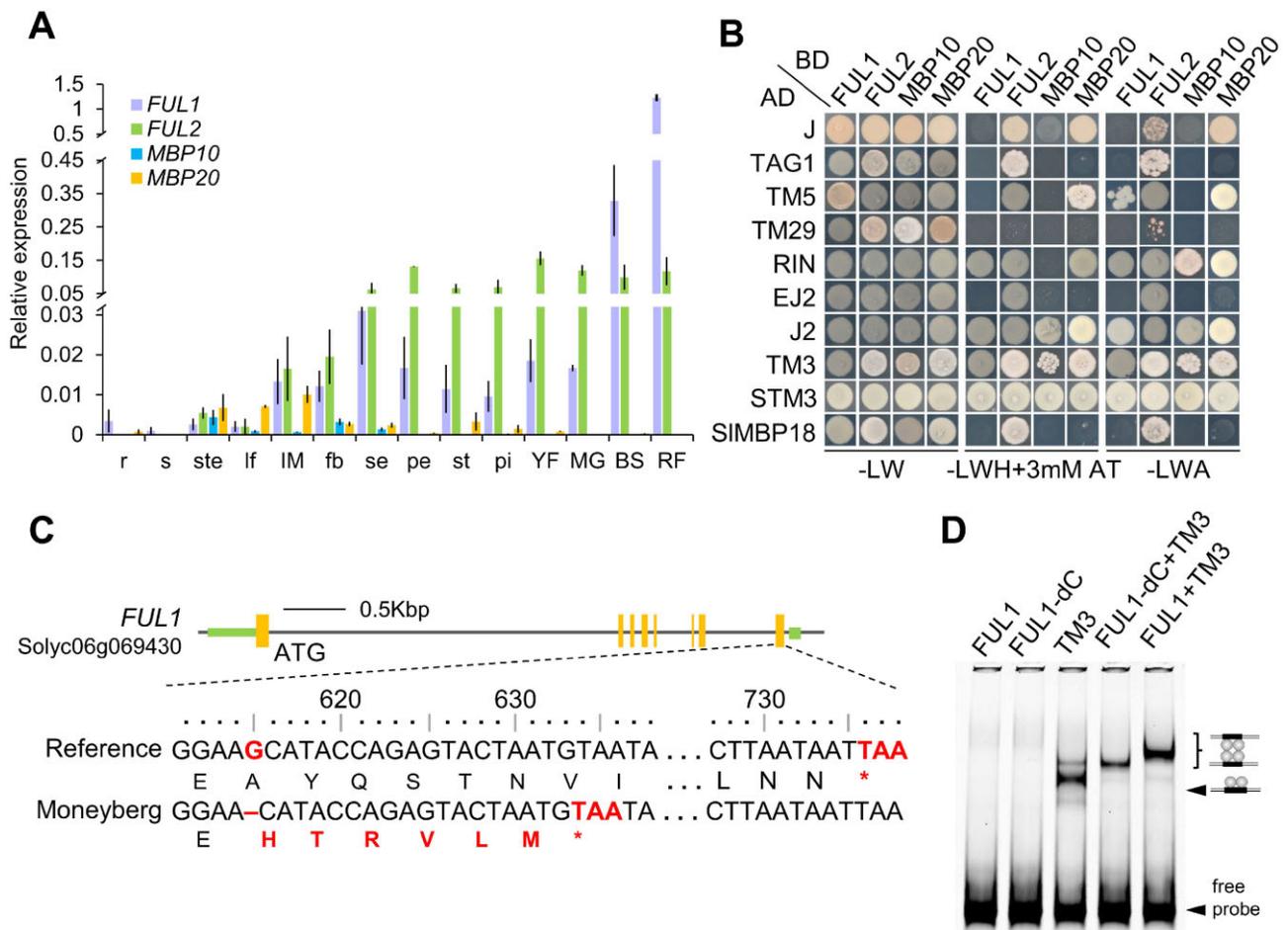
Figure 1 Characterization of the tomato *FUL*-like genes. A, Relative expression profiles of *SlFUL* genes in different organs obtained by RT-qPCR. r, 2-week-old root; s, 2-week-old shoot; ste, stem below apex; lf, young leaf; IM (dissected apex); fb, closed flower bud; se, sepal; pe, petal; st, stamen; pi, pistil; YF, young fruit; MG, mature green fruit; BS, breaker stage fruit; RF, red ripe fruit. The error bars indicate ±SD based on three biological replicates. B, Y2H assays showing the protein interactions of the FUL-like proteins with other tomato MADS-domain proteins. L, leucine; W, tryptophan; H, histidine; A, adenine; 3-AT, 3-amino-1,2,4-triazole. C, Location of the one-nucleotide deletion present at the 3′-end of the *FUL1* gene in the cultivar Moneyberg, resulting in a protein lacking the C-terminus. Orange rectangles indicate exons; green bars indicate UTRs. D, EMSAs showing that the FUL1 truncated protein (FUL1-ΔC) is functional in vitro.

interaction partners and MBP10 has the smallest set of interactors. The low number of interactors for MBP10 in combination with its weak overall expression pattern hints at relaxed selective pressure on this gene.

Different variants of the *FUL1* gene exist in tomato cultivars

Upon cloning and sequencing of the *FUL1* cDNA of tomato cv. Moneyberg, which was used in our experiments, we noticed a deletion of the 5th base (G) of the last exon as compared to the reference sequence (cv. Heinz). This deletion is predicted to result in a 205 amino acid protein, lacking the C-terminal 40 amino acids as compared to the reference (Figure 1, C). Inspection of the genome sequence of 38 resequenced cultivated tomato varieties (Consortium et al., 2014) showed that approximately half (17) contain this deletion (Supplemental Figure S2, A). The latter included the much-studied cv. "Ailsa Craig". The deletion was not detected in any of the re-sequenced wild accessions,

suggesting that it may have first emerged after domestication. Although the deletion results in a C-terminally truncated protein (FUL1-ΔC), no differences in interactions were observed in a Y2H assay (Supplemental Figure S2, B). An electrophoretic mobility shift assay (EMSA) also revealed that FUL1-ΔC can bind to a CArG-box-containing DNA fragment as a heterotetramer with TM3 (Figure 1, D). Thus, in vitro DNA-binding and protein–protein interaction capacities appear normal for FUL1-ΔC, indicating, together with the already described fruit ripening function for FUL1-ΔC in the cultivars Moneyberg and Ailsa Craig (Bemer et al., 2012; Wang et al., 2019), that the truncated protein is functional. To investigate whether there could be a link between the occurrence of the *FUL1-ΔC* allele and certain crop traits, we examined the recently published data set of Roohanitaziani et al. (2020), in which a wide variety of cultivars and wild species has been characterized for many traits, including flower/fruit abscission, flowering time, inflorescence architecture, fruit development, and fruit ripening.

However, we did not find significant differences in any of these traits between the cultivars with a full-length *FUL1* allele and those with a truncated allele (Supplemental Figures S2, C and D), suggesting that the occurrence of the *FUL1*-ΔC allele does not have a major influence on the investigated features.

FUL2 and MBP20 promote flowering in the primary and sympodial shoots

To dissect the biological roles of the *SlFUL* genes in planta, we generated loss-of-function single- and higher order mutants with the CRISPR/Cas9 method. The first coding exon of each gene was targeted with three single-guide RNAs. After stable tomato transformation of the cultivar Moneyberg, we screened several independent first-generation (T0) transgenic lines for the presence of insertion/deletion (indel) alleles by PCR and sequencing. Then we generated the progeny of the primary transgenics (T1) and selected two different homozygous indel alleles for each gene, encoding truncated proteins caused by frameshifts and premature stop codons (Supplemental Figure S3). T2 phenotyping of the selected mutants revealed that the plants with homozygous knock-out alleles for either *FUL2* or *MBP20* exhibited delays in primary shoot flowering, switching to reproductive growth after 13 leaves, compared with 11 in the WT (Figure 2, A). The number of days to first flowering was also significantly increased but was more variable between individuals of the same genotype (Supplemental Figure S4, A). No significant effect in the number of leaves was observed for the *ful1* or *mbp10* single mutants (Figure 2, A and Supplemental Figure S4, B). The observed delay in the transition to flowering was more pronounced in higher-order mutants, with approximately three leaves extra in *ful2 mbp20*, *ful1 ful2 mbp20*, and *ful1 ful2 mbp10 mbp20* compared with the WT (Figure 2, A). The fact that neither the *ful1* nor the *mbp10* mutations enhanced the mutant phenotype suggests that *FUL2* and *MBP20* are the most important *FUL*-like genes for promoting the floral transition. In addition to a delay in primary shoot transition, we also observed late flowering in the sympodial shoots of the same set of mutants, increasing to an average of four leaves per sympodial shoot, while the WT always has three (Figure 2, B and C; Supplemental Figure S4, C and D). To further investigate the delayed flowering phenotype, we imaged the primary shoot meristems of the WT and quadruple mutant at different leaf stages and determined their size, as well as the timing of the reproductive stage transition (Figure 2, D and Supplemental Figure S4, E and F). We did not observe differences in the size or shape of the meristems in the vegetative stage, but discovered that the timing of meristem doming differed. In the WT, meristem transition proceeded rapidly with a visible doming after formation of nine leaves. However, in the quadruple mutant, doming was initiated later and proceeded slower, resulting in development of the FM only after 12 leaves. In conclusion, *FUL2* and *MBP20* additively regulate the timing

of flowering in both the primary shoot and the sympodial shoots. Later during development, *ful1* single mutants also showed an increase in leaf number (Figure 2, B and Supplemental Figure S4, D), suggesting that *FUL1* plays a minor role as well.

FUL1, FUL2, and MBP20 control inflorescence architecture

We observed that the mutant plants had more branched inflorescences than WT plants, which typically produced only nonbranched inflorescences (Figure 2, E). We quantified the branching events for the first seven inflorescences of each plant in the T2 generation. Except for *mbp10*, all mutants showed increased inflorescence complexity, ranging from bi-parous to quintuple-parous inflorescences (Figure 2, F). Notably, 13.6% of the inflorescences from WT plants branched, while *ful1*, *ful2*, and *mbp20* lines produced 43.1%, 56.1%, and 50% branched inflorescences, respectively. In higher order mutants, branching increased further to ~75% in both the *ful2 mbp20* and the *ful1 ful2 mbp20* mutants. *mbp10* mutants were hardly branching, similar to the WT, while *mbp10 mbp20* mutants were identical to *mbp20* mutants. These results indicate no additional contribution of *mbp10* or *ful1* to the branching phenotype of the mutants. Surprisingly, the *ful1* mutant did exhibit enhanced branching, but its mutation did not further enhance the phenotype of the *ful2 mbp20* mutant, suggesting that *FUL1* function depends on *FUL2* and/or *MBP20* (Supplemental Figure S4, G). Interestingly, all first appearing inflorescences did not branch, except for the first inflorescence of *ful2 mbp20* (3 plants out of 11) and *ful1 ful2 mbp20* (2 plants out of 11). Higher order branching events (i.e. quintuple parous) were observed only in mutant lines where *ful2* was included, suggesting that *FUL2* has the most prominent role in the repression of inflorescence branching. We quantified the number of flowers on the second to fourth inflorescences. The more complex inflorescences developed more flowers, increasing from on average 10 in WT inflorescences to approximately 20 in the higher order mutants (Supplemental Figure S4, H). To investigate whether the increased branching could also be linked to delayed FM maturation, as observed for the *j2 ej2* (Soyk et al., 2017), *s* and *an* mutants (Lippman et al., 2008), we examined different stages of meristem development under the microscope (Figure 2, G). We observed delayed FM development of the sympodial shoot meristems, which initiated sepal primordia slower than the WT, allowing the formation of a second IM before FM maturation. We checked these observations with scanning electron microscope (SEM) pictures (Figure 2, H), which confirmed that meristem shape does not differ between the WT and quadruple mutant, but that the FMs of the mutant develop much slower. This is clearly visible in Figure 2, H, where the WT has already two FMs with initiated sepal primordia, while mutant FM development is delayed, allowing the formation of an additional IM, which is the earliest indication of branching. The frequency of
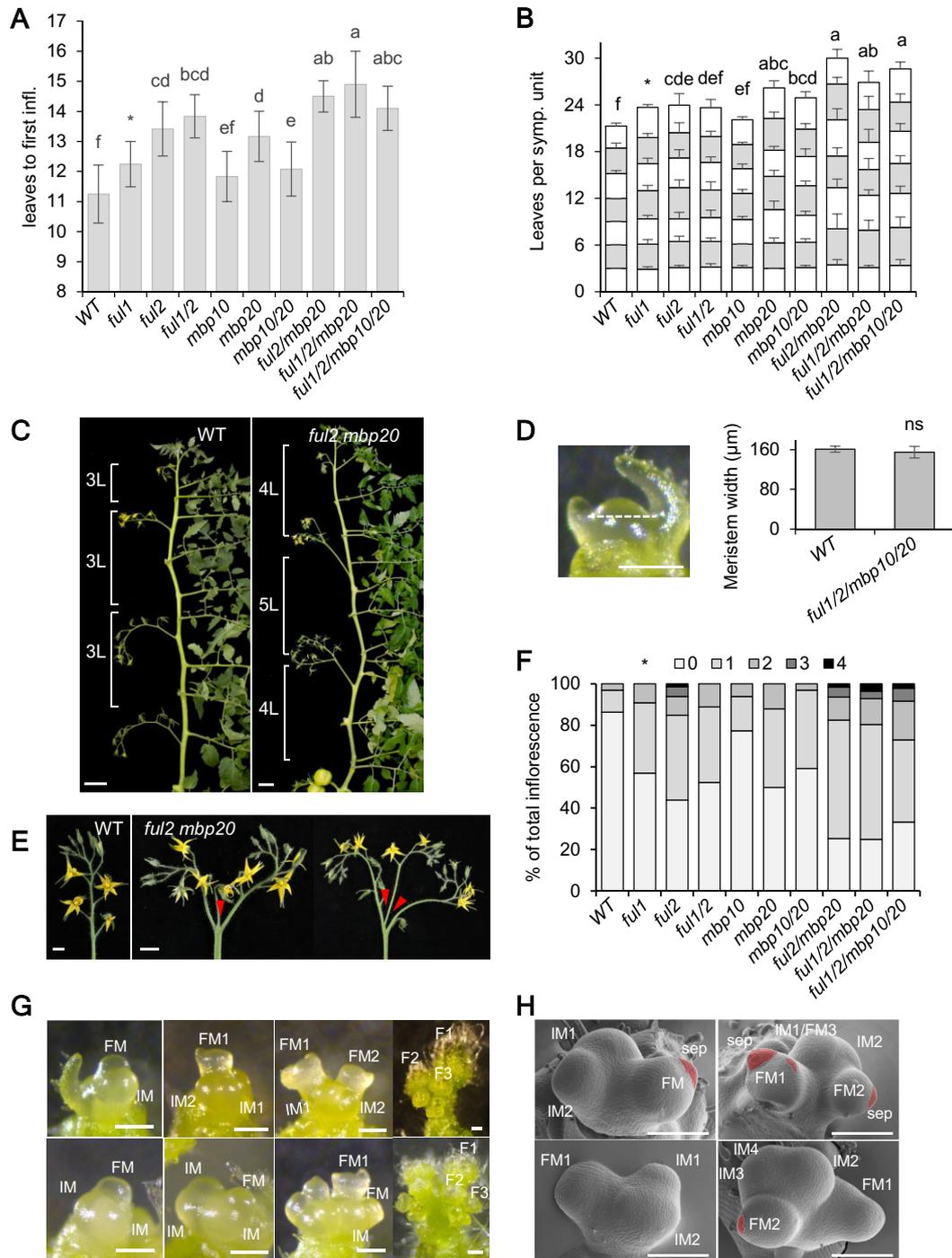
Figure 2 Disruption of the *FUL*-like genes results in delayed flowering and enhanced inflorescence branching. A, Quantification of primary shoot flowering for WT and *slful* mutants. B, Number of leaves per sympodial unit for the first seven units in WT and *slful* mutants. The average of the leaves per unit was used to test the significance. C, Representative sympodial shoots from WT plants and the *ful2 mbp20* mutant. L: leaf; Scale bars: 5 cm. D, Quantification of SAM width from WT and *quadruple* mutant plants. VMs were in the 10-leaf stage. The dashed line marks the width for measurement. ns, not significant. White bar: 200 μm. E, Representative images of WT and mutant (branched) inflorescences. Red arrowheads indicate branching events. Scale bars: 2 cm. F, Proportion of branched inflorescences per branching category for the indicated genotypes. The numbers (1–4) indicate the number of branching events. G and H, Developmental series of sympodial meristems of WT and quadruple mutant imaged by stereomicroscope (G) and by scanning electron microscope (H). In (G) and (H), the upper panels are from WT and the lower from quadruple mutants. In (H), developing sepal primordia are marked in red. F, flower; White bar: 200 μm. In (A) and (C), mean values ($\pm$SD) were compared between genotypes using one-way ANOVA followed by a post hoc LSD test, different letters indicate the difference at $P < 0.05$ level, six individual T2 offspring plants were analyzed per line and the data from the two different genotypes were combined for each mutant (e.g. 2 × 6 individuals for *ful1*, etc.). The asterisk in (A), (B), and (F) indicates that the *ful1* data were acquired from a second phenotyping experiment.

additional IMs was variable, but most similar to that of the *j2 ej2* mutant (Soyk et al., 2017). In conclusion, mutations in *FUL2* and *MBP20*, individually or combined, result in increased branching during inflorescence development. Both genes thus regulate inflorescence architecture in an additive manner, probably by regulating FM maturation. *FUL1* is also involved in this process as is shown by the *ful1* single mutant phenotype, but its role is masked in higher order mutants that contain *ful2* and *mbp20* alleles.

MBP10 and MBP20 do not contribute to fruit development and ripening

FUL1 and *FUL2* were reported as redundant regulators of tomato fruit ripening, and *FUL2* has an additional function in early fruit development (Bemer et al., 2012; Wang et al., 2019). Since *MBP20* is weakly expressed in carpels and early stages of fruit development (Figure 1, A), we wondered whether it could function in fruit development as well. We therefore examined fruit development and ripening in the different mutant lines. As reported previously, the *ful2* mutant fruits were smaller with stripes on the pericarp, while the *ful1 ful2* mutant fruits were more severely impaired in ripening (Wang et al., 2019). *ful2 mbp20* mutant fruits had the same phenotype as *ful2* fruits, while triple (*ful1 ful2 mbp20*) and quadruple fruits resembled *ful1 ful2* fruits in terms of width, Brix value, number of locules, pericarp stripes, and the overall external and internal appearance, indicating that *MBP10* and *MBP20* do not contribute to fruit development and ripening (Supplemental Figures S5, S6).

Remarkable was the high Brix values of fruits that contained *ful2* mutant alleles, although this may to a large extent be due to the smaller size of *ful2* fruits (Supplemental Figures S5, A and B). Interestingly, the number of locules was slightly, but significantly, enhanced in *ful2* single mutants, and in most mutant combinations that contained *ful2* (Supplemental Figure S5, C and D), suggesting that *FUL2* could have an additional role in the regulation of FM termination.

Dynamic expression of MADS-box genes in the meristem

The CRISPR mutant analysis revealed that *FUL2* and *MBP20* promote the transition from vegetative to reproductive development and control inflorescence architecture. To further unveil the role of the *SlFULs* in flowering, we conducted RNA-seq to compare the transcriptome dynamics during three consecutive stages (VM, TM, and FM) of meristem development between the WT and quadruple mutant. For each stage, over 30 meristems from a batch of plants were dissected and pooled for RNA extraction. Three independent batches were grown in the greenhouse at different time points to serve as biological replicates. For practical reasons, the FM and flanking IM were harvested together (further referred to as FIM) (see Figure 3, A). High-throughput sequencing yielded a minimum of 30M reads per sample. A PCA plot was generated of all 18 samples, which showed clear separation of the VM, TM, and FIM
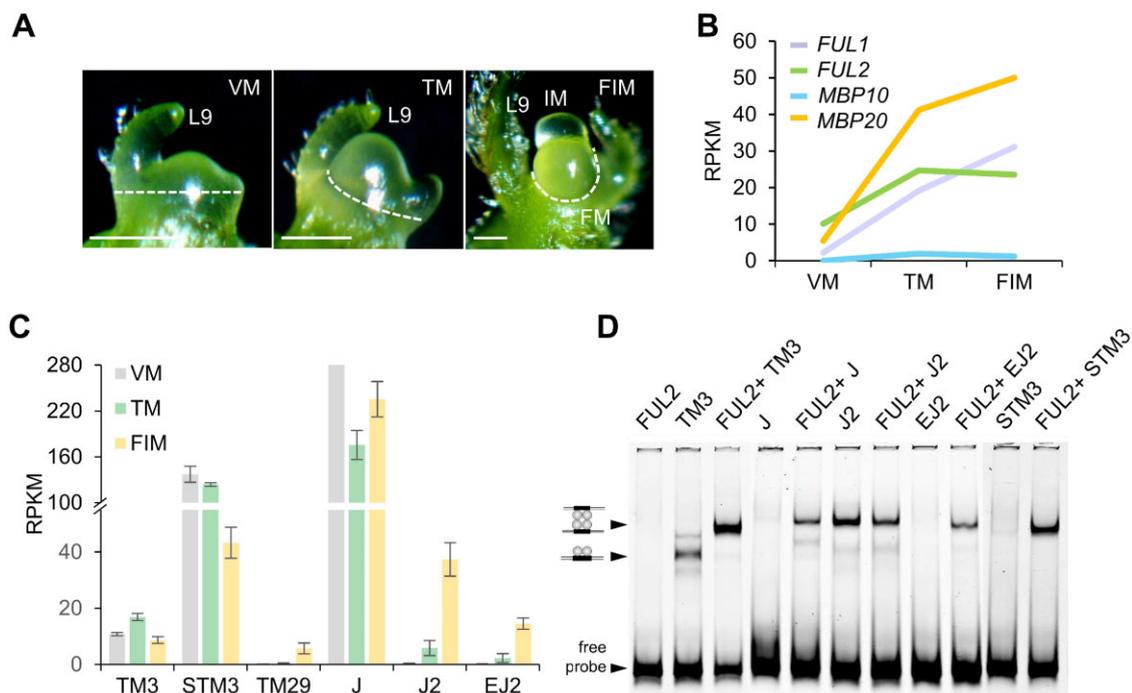

Figure 3 Gene expression dynamics in the primary shoot meristem. A, Manual microdissection of the three successive meristem stages of primary shoot meristems for transcriptome profiling. Dashed lines indicate the dissected tissues. White bar: 100 μm. B and C, Normalized gene expression (RPKM) of the *FUL*-like genes and *TM3*, *STM3*, *TM29*, *J*, *J2*, and *EJ2* in WT meristem stages. The values shown (mean ± SD) are the average of three replicates. D, EMSA assays showing FUL2 interactions with MADS-domain proteins. FIM: FM and IM.

samples, although there was quite some variation between the individual TM samples, probably reflecting the transient nature of this stage (Supplemental Figure S7, A). We first determined the expression of the *SlFULs* in the different stages of meristem development, revealing dynamic expression changes through the vegetative-to-reproductive transition for *FUL1*, *FUL2*, and *MBP20* (Figure 3, B). *FUL2* and *MBP20* are already expressed at the VM stage, but their expression highly increased in the TM stage. *FUL1* is more weakly expressed in the VM, but also reaches high expression levels in the TM and FIM. The higher expression of *FUL2* and *MBP20* in the VM stage is in line with their prominent role in the determination of flowering time. Of the MADS-box genes encoding SlFUL interactors, *J* was highly expressed in all three stages, while the expression of the *SEP*-like genes *EJ2*, *TM29*, and *J2* gradually increased from practically absent in VM to clearly expressed in FIM. The *SOC1*-homologs *TM3* and *STM3* were also expressed in all three stages (Figure 3, C), but their expression decreased in the FIM in contrast to that of *EJ2*, *TM29*, and *J2*. The other potential SlFUL interactors were only weakly expressed. To validate the RNA-seq data analysis, we confirmed the expression patterns of the *SlFULs*, and the genes encoding putative interactors, with RT-qPCR analysis on pooled meristem samples from independently grown batches (Supplemental Figure S7, C and D).

The combination of the expression and interaction data provides insight into the MADS-domain complexes that may act in planta. *J2* and *EJ2* are hardly expressed in the VM/TM, but considerable expression was detected in the FIM samples, which is probably the result of high FM expression, as detected by Park et al. (2012) (Thouet et al., 2012; Park et al., 2012; Alonge et al., 2020). Thus, FUL1, FUL2, and MBP20 probably form a complex with J2 and EJ2 in the FM to promote FM maturation. This is in agreement with the enhanced branching phenotype in *j2 ej2* mutants (Soyk et al., 2017). However, in the VM, where *J2* and *EJ2* are not expressed, FUL2 and MBP20 probably interact with the protein products of the abundantly expressed *TM3*, *STM3*, and *J* genes (Figure 3, C). To confirm that these complexes can be formed and bind to CArG-boxes in the DNA, we performed EMSA experiments with FUL2 or MBP20 and the putative interaction partners. Because MADS-domain proteins can only bind to the DNA probe as dimers or tetramers (De Folter et al., 2005; Immink et al., 2009), a shifted probe in the assay indicates that a dimer has been formed. Since FUL2 and MBP20 do not form homodimers (Figures 1, B, 3, D and Supplemental Figures S1, A, S7, E), we could in most cases confirm the formation of heterodimeric/tetrameric complexes by the gain of a probe shift. This was only problematic for the interactors that formed strong homodimers themselves (TM3 and J2), but for TM3, the addition of FUL2 or MBP20 resulted in a clear shift towards a tetrameric complex, confirming the Y2H data as well (Figure 3, D

and Supplemental Figure S7, E). Thus, based on expression patterns of the genes and interaction capacity, FUL2 and MBP20 probably interact with TM3/STM3 and J in the VM to regulate flowering time, while it is plausible that FUL1, FUL2, and MBP20 form a complex with J2 and EJ2 to promote FM maturation. In addition, FUL1 and FUL2 may interact with the less abundant TM29 for this purpose.

Identification of differentially expressed genes

Comparison of WT and quadruple mutant transcriptomes revealed 130 differentially expressed genes (DEGs) for the VM stage (103 up- and 27 downregulated in the mutant), 125 for the TM stage (103 up- and 22 downregulated), and 216 DEGs for the FIM stage (182 up- and 34 downregulated), using FDR-corrected $P < 0.05$ as a threshold for significance and a Log_2 fold change > 1.0. These genes significantly overlapped between stages, with 23 genes differentially expressed in all three stages (Supplemental Figure S7, B). Many more genes were upregulated in the mutant than there were downregulated, pointing toward a general repressive function of SlFUL-containing complexes, in agreement with the data from Arabidopsis *FUL* studies (Ferrándiz et al., 2000; Bemer et al., 2017; Balanzà et al., 2018). A large proportion of the DEGs are involved in metabolic processes, such as terpene synthesis or the phenylpropanoid pathway, but the corresponding genes were in general weakly expressed in the meristem (Supplemental Data Set S1). Notably, the phenylpropanoid pathway is also controlled by *FUL1/2* in tomato fruits (Bemer et al., 2012), indicating that the regulation of some identified DEGs is probably of greater importance in other tissues. The DEG lists also contained several interesting genes that are possibly involved in flowering, although previously described tomato key regulators, such as *AN*, *FA*, *SFT*, *SP*, and *S* were not among the DEGs (Supplemental Data Set S1). We searched the list of DEGs for genes that may explain the flowering phenotypes instead, and identified a few homologs of known Arabidopsis flowering genes, such as *VRN1* and *AHL15*, which are involved in the regulation of flowering time and axillary meristem outgrowth, respectively (Levy et al., 2002; Karami et al., 2020). Also, the MADS-domain factors *TM3* and *SlMBP13* were significantly upregulated in the quadruple mutant in all three meristem stages. Most interestingly, however, is the identification of four CK signaling genes as targets of the *SlFULs*.

The SlFUL proteins repress negative regulators of CK signaling

Compelling evidence shows that CK is required for SAM activity and FM initiation, and that the interplay of transcription factor regulation and CK signaling controls SAM size and activity (Kurakawa et al., 2007; Bartrina et al., 2011; Han et al., 2014). Moreover, a recent report showed that the CK reporter TCSv2 is highly expressed in tomato reproductive meristems (Steiner et al., 2020). In our list of DEGs, we identified several genes involved in CK signaling, namely three *CKXs*, *CKX5/6/8* (naming according to Matsuo et al., 2012),

and one type-A ARABIDOPSIS RESPONSE REGULATOR (ARR), ARR16. CKXs irreversibly degrade active CKs and type-A ARRs function as negative regulators of the CK response (Brownlee et al., 1975; McGaw and Horgan, 1983; D'Agostino et al., 2000). CKX6 and CKX8 were upregulated in the VM and TM stages of the mutant, but not in the FIM stage, while CKX5 and ARR16 were only upregulated in the TM stage (Figure 4, A). We confirmed their differential expression with RT-qPCR in independent samples (Supplemental Figure S8, A). Therefore, the upregulation of CKX5/6/8 and ARR16 in the VM and TM stages will probably result in a reduced CK content and responsiveness. We further investigated whether FUL2 and MBP20 can directly repress CKX/ARR gene expression by binding to their promoters. We therefore scanned the up- and downstream regions of the CKX/ARR genes for CArG-box motifs, the binding sites for MADS-domain proteins (Kaufmann et al., 2009; Aerts et al., 2018). Putative CArG-boxes were present in all differentially expressed CKX/ARR genes (Supplemental Figure S8, B). To test whether FUL2 and MBP20 can bind to these motifs, we performed EMSAs using fragments containing these CArG-boxes as native probes. Because MADS-domain proteins need to form a dimer to bind to the DNA, we tested TM3-FUL2 and TM3-MBP20 heterodimers, as these proteins form strong heterodimers in yeast and are probably interacting in the VM/TM. In addition, as shown above (Figure 3, D), the FUL2/MBP20-TM3 tetrameric complex can be easily distinguished from the TM3 homodimeric complex in EMSA assays. We detected clear shifts for all tested regulatory fragments (Figure 4, B), suggesting that the FUL2-TM3 and MBP20-TM3 heterodimers can physically bind to the tested CKX/ARR genes. To investigate whether the CArG-box is essential for the binding, we also generated mutated probes, in which the CArG-box was mildly perturbed by a single-nucleotide mutation in the center of the motifs. This probe mutation abolished or reduced the binding in all cases except for CKX5 (Figure 4, B), confirming the importance of the CArG box for the binding of the heterodimers. To determine whether FUL2 and MBP20 both play a role in repressing the CK signaling genes, we harvested meristems from ful2 and mbp20 single mutants and performed RT-qPCRs to determine the upregulation of the CKX/ARR genes. Upregulation was visible in both single mutants but was in the VM stage more distinct in the ful2 mutant than in the mbp20 mutant (Figure 4, C), in line with the higher expression of FUL2 at this stage (Figure 3, B). In the TM stage, both mutants showed a similar mild upregulation. The upregulation in the single mutants was considerably weaker than in the quadruple mutant, reflecting the partially redundant functions of both genes. To test our hypothesis that the late primary shoot flowering in the quadruple mutant is due to delayed doming as a result of impaired CK accumulation, we investigated the CK activity in the meristem of WT Moneyberg plants using the TCSv2:GUS reporter (Steiner et al., 2016). At the apex of the primary shoot, the CK signal was low in the early and late VM stage, but

intense in the TM stage (Figure 4, D), indicating that an accumulation of CK had occurred, probably inducing meristem doming. To test whether CKX activity could indeed influence flowering time, we created two independent CRISPR mutants for the highest expressed gene, CKX6, and compared the flowering time of the homozygous T1 mutants with that of the WT (Supplemental Figure S8, C and Figure 4, E). The ckx6 mutant showed a mild, but significant acceleration of flowering time, consistent with a role of CKX genes in the regulation of TM development right after the initiation of transition by upstream flowering signals. These results suggest that both FUL2 and MBP20 directly bind to the promoters of the CKX5/CKX6/CKX8 and ARR16 genes to repress their expression and thereby upregulate CK signaling in the VM at the start of the transition to flowering.

Identification of downstream genes involved in the repression of branching

Searching for DEGs potentially involved in the flowering phenotype of the quadruple mutant, we found very few genes that could be associated with the inflorescence branching phenotype. However, as mentioned above, the primary shoot FIM, which was harvested for the RNA-seq, only rarely gave rise to branched inflorescences. Ubiquitous branching in the quadruple mutant was only observed in the inflorescences of the sympodial units, from the first sympodial unit onwards. Therefore, we performed an additional RNA-seq experiment to compare the transcriptomes of WT and quadruple mutant, harvesting the same mixed FM/IM from the sympodial shoot as sampled for the primary shoot, designated SFIM (Supplemental Figure S9, A). This experiment, with the same set-up as described above, revealed 121 DEGs, of which 96 were upregulated and 25 downregulated in the quadruple mutant. Previously reported key regulators of branching, such as S, FA, and AN, were not in the list of DEGs. The expression of the SP gene, which suppresses the reproductive transition of the sympodial shoot meristem (Pnueli et al., 1998; Thouet et al., 2008), was remarkable, as it varied considerably between samples (Supplemental Figure S9, B). To identify genes possibly responsible for the inflorescence branching, we searched for flowering-related genes that were differentially regulated in the SFIM samples, but not in the FIM samples (Figure 5, A). Four transcription factors were identified that may be involved in the regulation of FM maturation: APETALA 2b (AP2b) (Karlova et al., 2011), AP2c, AGL6, and TM29 (Figure 5, B). Only for AP2b, the differential expression could be confirmed by RT-qPCR in independent samples (Supplemental Figure S9, C). AP2-like genes are angiosperm-wide regulators of both meristem development and flowering, controlling for example stem-cell maintenance in the Arabidopsis SAM (Würschum et al., 2006), and floral and spikelet meristem initiation/termination in maize (Zea mays L.) (Chuck et al., 2008), in addition to their "floral" roles in sepal/petal development and repression of the C-function
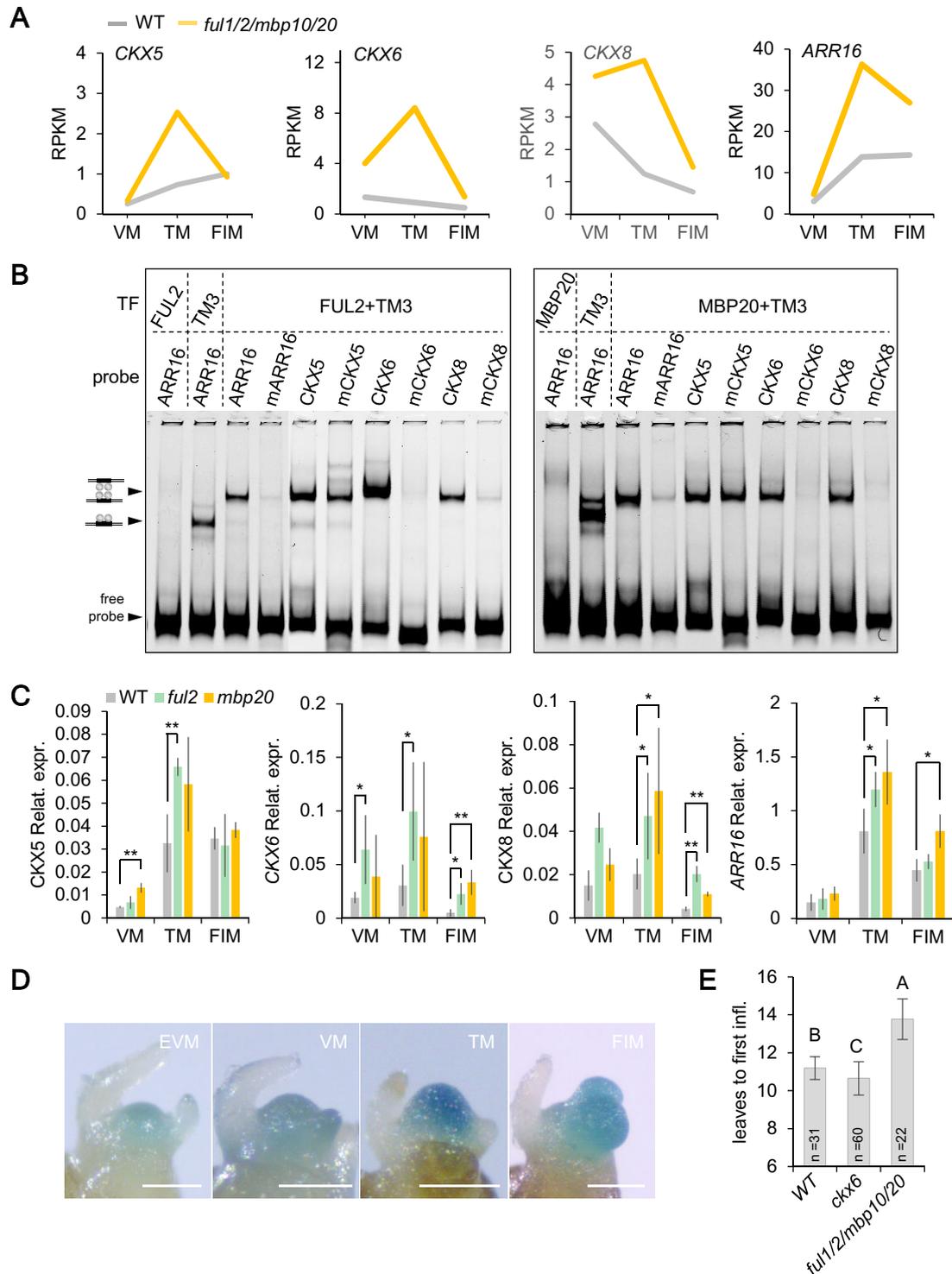
Figure 4 FUL2 and MBP20 regulate *CKX5/6/8* and *ARR16* expression. A, Normalized gene expression (RPKM) for *CKX5/6/8* and *ARR16* across vegetative and reproductive meristem stages. B, EMSAs showing that FUL2-TM3 directly binds to promoter fragments of *CKX5/6/8* and *ARR16* in vitro. The arrow indicates the shift of the probe caused by the binding of FUL2-TM3. The mutated versions of the promoter fragments are indicated with an "m." TF, transcription factor. C, Expression of *CKX5/6/8* and *ARR16* during SAM transition in WT, *ful2*, and *mbp20* obtained by qRT-PCR. D, GUS staining of TCSv2::GUS in meristems during floral transition. E, Quantification of primary shoot flowering for WT, *ckx6*, and *slful* quadruple mutant plants. n, number of individual plants. In (C), the values shown (mean ± SD) are the average of three replicates. Significant differences were calculated using one-tailed Student's *t* test (*$P \leq 0.05$ and **$P \leq 0.01$) in (C), and one-way ANOVA followed by a post hoc LSD test in (E), and different letters indicate the difference at $P < 0.01$ level. EVM, early VM.
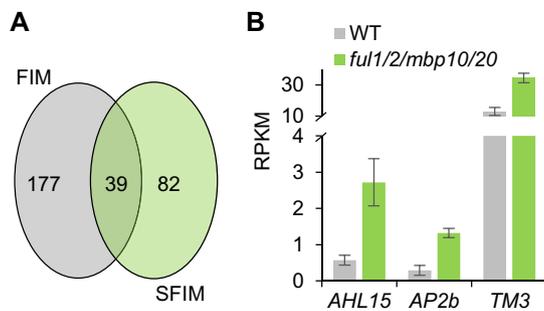
A

FIM

B

Figure 5 Gene expression in floral meristems of the sympodial shoot in WT and *slful* quadruple mutants. A, Venn diagram showing the overlap of DEGs in the IM/FM (FIM) of primary shoot and sympodial shoot (SFIM). B, Normalized gene expression (RPKM) of DEGs of interest in WT and quadruple mutant SFIM. The values shown (mean ± SD) are the average of three replicates.

(Yant et al., 2010; Morel et al., 2017). In addition to these specifically DEGs, two other genes that are also upregulated in the primary shoot FM, but to a lesser extent (Supplemental Data Set S1), are probably candidates to explain the branching phenotype as well. Mutation of the first one, *TM3*, results in reduced inflorescence branching in the *ej2 j2* mutant background, implying that higher expression of *TM3* will cause enhanced branching (Alonge et al., 2020). The other gene is a close homolog of Arabidopsis *AHL15*, which suppresses axillary meristem maturation (Karami et al., 2020). If tomato *AHL15* is also repressing meristem maturation, this could contribute to the enhanced branching phenotype. In conclusion, *FUL1*, *FUL2*, and *MBP20* do not seem to regulate inflorescence branching by modifying the expression of the key regulators *S*, *FA*, or *AN*, but we identified several other downstream transcription factors that may be involved.

FUL1 expression is regulated by FUL2 and MBP20

Despite the high expression of *FUL1* in the TM and FIM and the branching phenotype in the *ful1* single mutants, the *ful1* mutation does not enhance the branching phenotype of the *ful2 mbp20* mutant (Figure 2, E and Supplemental Figure S4, G). The considerable downregulation of *FUL1* in the quadruple mutant may explain this apparent discrepancy (Figure 6, A and Supplemental Figure S10, A), and indicates that the gene is induced by FUL2, MBP20 and/or by itself via a positive (auto-)regulatory loop. Because the expression of *FUL1* is low in the VM, FUL2-, and/or MBP20-containing complexes may need to bind to the CArG-boxes in the *FUL1* regulatory region to upregulate its expression in TM and FM/IM. To test this and determine the separate effects of FUL1, FUL2, and MBP20 on *FUL1* regulation, we performed RT-qPCRs in the corresponding single mutants (Figure 6, B). Downregulation was observed in all three single mutants, particularly in the FIM stage, but the transcript reduction was most severe in the *ful1* mutants. The lower *FUL1* mRNA level in the *ful1* mutant may be caused by nonsense-mediated mRNA decay as a result of the premature stop

codon. However, it could also be the result of abolished *FUL1* autoregulation, or a combination of both decay and disturbed autoregulation. At this point, we cannot discriminate between these possibilities. It is clear, however, that both FUL2 and MBP20 positively regulate *FUL1* expression. There are four CArG-boxes in the upstream region of *FUL1* that can probably be bound by MADS-domain complexes (Supplemental Figure S10, B). To test whether FUL2 and MBP20 can bind, we performed EMSAs with TM3-FUL2 and TM3-MBP20 dimers and observed clear binding to the CArG-box containing probes (Figure 6, C), suggesting that *FUL1* depends on FUL2 and/or MBP20 for maximal expression in the TM and FM stages.

Discussion

Subfunctionalization of the *SlFUL* genes

Following segmental or whole-genome duplication events, genes with new molecular functions can arise through sub- or neofunctionalization, resulting in divergence of biological functions. We show here that functional divergence also occurred for the *SlFULs* after their multiplication early in the Solanaceae lineage. In addition to their previously described roles in fruit development and ripening (Bemer et al., 2012; Wang et al., 2019), we unveil that *FUL1* and *FUL2* both regulate FM/IM development, albeit at different levels. *MBP20* regulates flowering together with *FUL2* but does not contribute to fruit development. We did not observe any phenotype for the *mbp10* mutant, nor did the mutation enhance the phenotype in higher order mutants. This suggests, together with its weak overall expression pattern and low number of protein–protein interactions, that *MBP10* may become a pseudogene. In line with this, *MBP10* lacks regulatory sequences in its first intron (Maheepala et al., 2019), and has a three amino acid mutation in the I-domain, a region important for protein–protein interactions (Van Dijk et al., 2010). The loss of *MBP10* in other Solanaceae genera such as *Petunia* also hints in this direction (Maheepala et al., 2019).

Although previous overexpression studies suggested that *MBP20* functions in leaf development and *FUL2* in stem development and secondary growth (Burko et al., 2013; Wang et al., 2014a; Shalit-Kaneh et al., 2019), we did not observe aberrant phenotypes in these tissues in our knockout mutants. The most probable explanation for this discrepancy is the use of the Cauliflower 35S promoter in the previous experiments (Wang et al., 2014a; Shalit-Kaneh et al., 2019), resulting in ectopic expression and misregulation of target genes at a position where *FUL2* and *MBP20* are usually not expressed. Overexpressing MADS-domain proteins or dominant-negative forms of MADS proteins can also perturb/block complexes of interaction partners in other tissues, leading to more severe phenotypes. However, another possibility is that *FUL2* and/or *MBP20* function redundantly with other MADS proteins in the investigated tissues. *AtFUL* and *SOC1* act redundantly in the regulation of secondary growth (Melzer et al., 2008), and *FUL2* may thus function
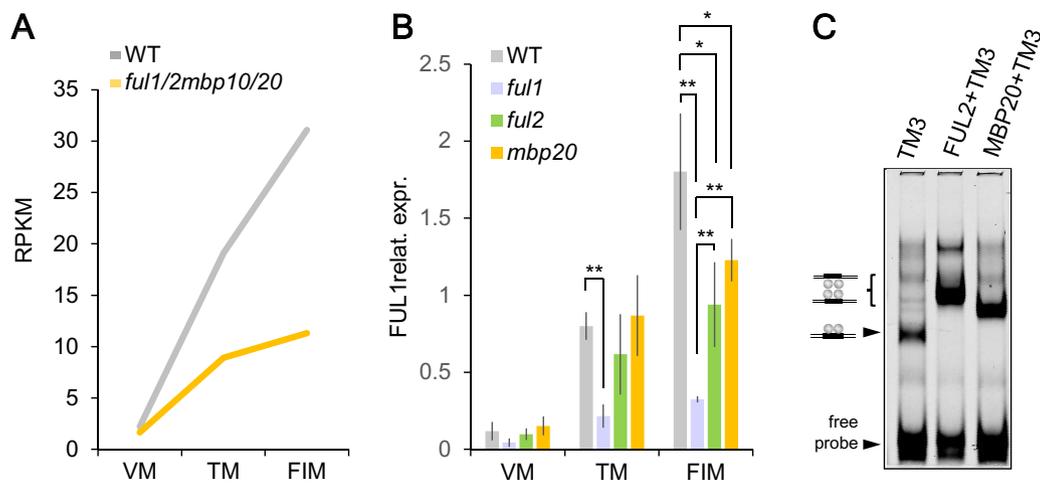
Figure 6 FUL2 and MBP20 regulate *FUL1* expression. A, Normalized gene expression (RPKM) of *FUL1* across vegetative and reproductive meristem stages in WT and quadruple mutant. B, FUL1 expression during SAM transition in WT, *ful1*, *ful2*, and *mbp20* tested by qRT-PCR. C, EMSA assays showing that FUL2/TM3 and MBP20/TM3 directly bind to the promoters of *FUL1* in vitro. The arrow indicates the shift of the probe caused by the binding of FUL2-TM3 or MBP20/TM3. The values shown (mean ± SD) are the average of three replicates. Significant differences were calculated using one-tailed Student's *t* test (*$P \leqslant 0.05$ and **$P \leqslant 0.01$).

redundantly with (S)TM3 in the tomato stem as well. In conclusion, the four *SlFULs* underwent a functional divergence during evolution, but together retained functions in both inflorescence and fruit development. It is possible that some functions have remained unidentified due to redundancy with other MADS-box genes.

The position of *FUL1* in the flower regulatory network

FUL1 appears to act differently from *FUL2* and *MBP20* in the meristems. It is only weakly expressed in the VM, and its high expression in TM and FM probably depends on *FUL2* and *MBP20*, which are already expressed earlier in the VM and can bind to the *FUL1* promoter. (Auto-)regulatory loops are a common phenomenon in MADS-box gene regulation. For example, Arabidopsis *AP1* contains a CArG-box in its promoter, which can be bound by its own protein as well as by its paralog (*CAL*) to achieve high expression levels throughout different stages (Ye et al., 2016). Because of the delayed induction, *FUL1* does not regulate flowering time, but does contribute to the repression of inflorescence branching.

Interestingly, we found that *FUL1* has a premature stop codon at the C-terminus in the cultivar Moneyberg and many other cultivars. Although this truncation does not alter in vivo dimer formation with other MADS-domain proteins (Supplemental Figure S2, B), nor disturbs tetramer formation and DNA binding (Figure 1, D), the C-terminus may be important for protein activity. It contains the highly conserved, but uncharacterized, FUL-specific PQWML motif (Litt and Irish, 2003). Arabidopsis *ful* mutants complemented with a FUL copy with a mutation in this motif, were less able to rescue the silique phenotype than those transformed with a WT copy, suggesting that the motif is important for protein activity (McCarthy et al., 2015).

Interestingly, the truncated allele has not been observed in wild relatives of tomato, and so probably first occurred after domestication (Supplemental Figure S2, A). We did not find a correlation, however, between the presence of the *FUL1*-Δ*C* allele and any trait characterized by Roohanitaziani et al. (2020), but we cannot exclude that the allele has been selected during breeding, for example by conferring slightly larger inflorescences without severe branching.

The role of *FUL2* and *MBP20* in the tomato flowering network

Several previously identified tomato flowering genes were revealed to be functional homologs of Arabidopsis flowering genes, such as *SFT* (*FT*) and *FA* (*LFY*) (Molinero-Rosales et al., 1999, 2004; Lifschitz et al., 2006), indicating that at least part of the Arabidopsis flowering network is conserved in tomato. However, the knowledge of the regulatory network underlying the tomato sympodial flowering pathway is still fragmented and it is yet unclear whether homologs of many important players in Arabidopsis, such as *SOC1* and *FLC*, are important for tomato flowering as well. Here, we show that tomato *FUL*-like genes regulate flowering and inflorescence development in tomato, thereby adding a piece to the tomato flowering network puzzle. In Arabidopsis, *FUL* is a target of FLOWERING LOCUS D (FD)/FT and SQUAMOSA PROMOTER BINDING PROTEIN-LIKE (SPL) proteins in the photoperiod pathway and the age pathway (Kardailsky et al., 1999; Wang et al., 2009; Jung et al., 2016), and functions partially redundantly with *AP1* in the promotion of flowering (Ferrándiz et al., 2000). We demonstrate here that *FUL2* and *MBP20* additively promote flowering similar to their homolog in Arabidopsis, but it is yet unclear whether they act downstream of SFT and the tomato SPLs as well. Within our set of DEGs, we did not identify any of the previously identified flowering regulators (e.g. FA, S, SFT,

SP), further indicating that the *SlFULs* may act downstream of, or parallel to, these factors.

MADS-domain transcription factors bind to the DNA as dimers (De Folter et al., 2005), and since the SlFUL proteins cannot form homodimers, they need to heterodimerize with other MADS-domain proteins to regulate target gene expression. For the regulation of flowering time, FUL2 and MBP20 probably form a complex with TM3, STM3, and J, because the corresponding genes are highly expressed in the VM/TM, and both *tm3 stm3* and *j* mutants display a small delay in flowering time (Szymkowiak and Irish, 2006; Thouet et al., 2012; Alonge et al., 2020) similar to *ful2* and *mbp20*.

Downstream of the *SlFULs*, we discovered several repressors of the CK pathway that are upregulated in the VM and TM stages of the quadruple mutant, probably resulting in reduced CK levels and signaling. In many species, the switch from vegetative growth to reproductive development is accompanied by cell division in the meristem, which results in meristem doming of the TM. We showed that this doming in tomato is accompanied by a high CK signal in the meristem, in agreement with the data of Steiner et al. (2020). This suggests that CK can positively regulate cell division during SAM doming to allow transition of the meristem. In line with this hypothesis, the reduced CK levels may inhibit SAM doming and thereby delay flowering. In Arabidopsis, CK deficiency through the overexpression of *CKXs* diminishes SAM activity and indeed retards flowering (Werner et al., 2003). In addition, initiation of both the axillary meristem and the FM were shown to require a CK signaling (Han et al., 2014; Wang et al., 2014b). We show here that the tomato *CKX6* gene is also repressing flowering, and that its mutant displays early flowering, probably due to faster accumulation of CK in the meristem. The observed acceleration of flowering was mild, which can be explained by the role of the *CKX* genes downstream of key flowering regulators. Other CK repressors, such as *CKX8*, which is also expressed in VM and TM (Figure 4, A), may have a partial redundant function and may increase the mutant phenotype when mutated in the *ckx6* mutant background. We did not further investigate the role of the *ARR16* gene, but its upregulation in the quadruple mutant may also add to impaired CK signaling and delayed TM development. In conclusion, our data provide evidence that *FUL2* and *MBP20* promote flowering through indirect regulation of CK levels by directly repressing *CKX* genes in the VM and TM (Figure 7).

In other species, such as Arabidopsis and Petunia (*Petunia hybrida*), *AP1/FUL*-like genes are involved in the establishment of FM/IM identity, and combinatorial mutations result in a loss of identity, leading to a non-flowering phenotype. The Arabidopsis *ap1 cal* double mutant forms only IMs, because FM identity is lost, and additional mutation of *ful* aggravates this phenotype, leading to more vegetative structures (Ferrándiz et al., 2000). In Petunia, the four *FUL/AP1* genes appear to function redundantly in the establishment of FM/IM identity, and higher order mutants remain for a
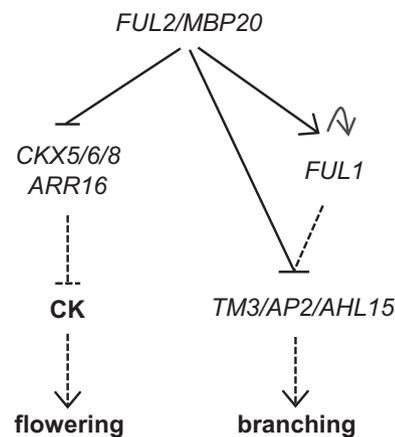

Figure 7 Model of SlFUL regulation of flowering time and inflorescence branching in tomato. The connections between the different regulators are based on the results of this study and other work described in the text. Solid lines display confirmed interactions, while dashed lines represent putative interactions.

long time in the vegetative stage (Morel et al., 2019). In tomato, vegetative reversion occurs after a few flowers have formed in mutants of *MC* and *J*, suggesting that they are required for IM fate as well (Szymkowiak and Irish, 2006; Thouet et al., 2012). We observed this phenotype only occasionally in the *slful* mutants, suggesting that the promotion of IM fate is mainly regulated by *J* and *MC*. It is possible, however, that the *SlFULs* act redundantly with *MC*, which would reflect the situation in Petunia.

The role of the *SlFULs* in the regulation of inflorescence architecture

We show that loss of function of *FUL1*, *FUL2*, and/or *MBP20* results in a branched inflorescence that produces an increased number of flowers. The phenotype is variable; however, with some mutant inflorescences staying single-parous, while others form up to five branches. Our transcriptome analysis revealed that this branching is not caused by regulation of *S*, *AN*, or *FA*, indicating that they function upstream of, or in parallel with, the SlFUL-containing complexes. Remarkable was the varying expression of *SP*, which may be involved in branching by the maintenance of IM identity (Supplemental Figure S9, B). A probable explanation for this variation is variable SYM outgrowth in the leaf axils of the sampled meristems, although approximately 30 meristems were pooled for each sample. Because the branching phenotype is also highly variable, we cannot exclude that *SP* is somewhat regulated by the *SlFULs* in FM/IM, thereby exerting an effect on the branching phenotype. This would be similar to the repression of the legume *TFL1*-homolog by the euFULII clade proteins VEG1 (pea) or MtFUL1-c (Medicago) (Berbel et al., 2012; Benlloch et al., 2015; Cheng et al., 2018; Zhang et al., 2021). The branching phenotype of the quadruple mutant resembles that of the *j2 ej2* mutant (Soyk et al., 2017) and our microscopic analysis suggests that it is caused by delayed maturation of the FM as well.

Given our in vitro interaction data, which show that the SlFULs can interact with J2 and EJ2, it is plausible that they act together in a complex to promote FM maturation and suppress inflorescence branching. Both *FUL1/FUL2/MBP20* and *J2/EJ2* are clearly expressed in the FIM in our data (Figure 3, C), although our sampling method did not allow a clear distinction between FM and flanking IM. However, the data from Park et al. (2012) are based on FMs that were completely isolated, and they describe high expression for *FUL1* and *FUL2* in the FM, while Soyk et al. (2017) describe the same for *J2* and *EJ2*, in agreement with an important role of a FUL1/FUL2/MBP20-J2/EJ2 complex in the regulation of FM maturation. Genetic experiments revealed that the *j2 ej2* mutant phenotype is additive to that of *s*, indicating that *J2* and *EJ2* function separately from the *S* gene (Soyk et al., 2017), and the same probably accounts for the *SlFULs*.

To identify genes downstream of the *SlFULs* that could explain the branching phenotype in the quadruple mutant, we performed transcriptome analysis in the FM/IM of the first sympodial unit. Our transcriptome analysis of the SFIMs unveiled several genes encoding transcription factors that were not differentially regulated in the FIM, or to a much lower extent. Since we observed the branching phenotype a few times in primary inflorescences of higher order mutants, the DEGs that were more prominent in the SFIM compared with the FIM, *TM3*, and *AHL15*, could explain the higher frequency of branching in the sympodial shoot inflorescences by a dosage effect. *TM3* is an interesting candidate, because its expression is high in VM and TM, but drops in FIM. This suggests that TM3 is repressing FM maturation, in line with the observation that the *tm3 stm3* double mutation represses the enhanced branching phenotype of *j2 ej2* (Alonge et al., 2020). The upregulation of *TM3* will thus delay FM maturation and thereby enhance branching. Indications for the involvement of the other genes, *AHL15* and *AP2b*, rather come from research in Arabidopsis and maize. In Arabidopsis, *AHL15* represses meristem maturation in the axillary buds (Karami et al., 2020), while *AP2*-like genes regulate meristem development in both Arabidopsis and maize (Würschum et al., 2006; Chuck et al., 2008). Which of these downstream factors is most important for the increased-branching phenotype still needs to be determined with future genetic experiments and localization studies to establish what their function is in either the FM or the IM.

Materials and methods

Plant materials and growing conditions

Tomato cv. Moneyberg was used for the *Agrobacterium tumefaciens*-mediated transformation experiments (Van Roekel et al., 1993). Tissue culture was conducted in a growth chamber with 16-h light and 8-h dark at 25°C. Plates were placed on shelves with either Philips TL 830 light tubes or Luxalight LED strips Neutral White 4300K, both with a light intensity of 60 μE at the plate level. After rooting, the plants were transformed to rockwool blocks,

watered with 1 g·L^{-1} Hyponex solution and cultivated in a 21°C growth chamber (16-h light/8-h dark) under similar light conditions (light intensity of 70 μE). Twenty-five-day-old plants were moved to the greenhouse and grown under ambient temperatures and natural light, supplemented with artificial sodium lights.

RT-qPCR analysis

For RT-qPCR analysis of *SlFULs* expression, root, shoot, leaves, flower organs, and fruits of different stages were harvested from WT tomato plants. RNA was extracted with a CTAB/LiCl method (Porebski et al., 1997), DNase treated with Ambion Turbo DNase (AM1907) and cDNA was synthesized with the iScript cDNA synthesis kit (Bio-Rad). Real-time PCR was performed with the iQ SYBR Green Supermix from Bio-Rad with a standard two-step program of 40 cycles, annealing at 60°C. Primer efficiencies were tested beforehand and only primer pairs with equal efficiencies were compared. *CAC* was used as a reference gene (all primer sequences are listed in Supplemental Table S1).

Yeast two-hybrid

Protein–protein interaction assays in yeast were performed using the GAL4 System using Gateway vectors as described (De Folter and Immink, 2011). The coding sequences for bait proteins and prey proteins were cloned into the pDEST32 and pDEST22 vectors respectively, and the vectors were transformed into the PJ69-4A and PJ69-4α yeast strains. The interaction screen was performed using -LWH dropout medium, supplemented with 3-mM 3-amino-1,2,4-triazole (3-AT) or -LWA dropout medium. Plates were incubated for 5 days at room temperature. All primer sequences used for cloning are listed in Supplemental Table S1.

CRISPR construct generation and stable tomato transformation

The *ful2* and *ful1 ful2* transgenic CRISPR lines have been previously generated (Wang et al., 2019). The constructs for all other lines were generated using GoldenGate cloning and the MoClo toolkit according to Weber et al. (2011). Briefly, each gRNA was fused to the synthetic U6 promoter as U6p:gRNA, and cut-ligated in a Level 1 vector. Level 1 constructs pICH47732-NOSpro:NPTII:OCST, pICH47742-35S:Cas9:NOST, pICH47751-35S:GFP:ter35S, pICH47761-gRNA1, pICH47772-gRNA2, pICH47781-gRNA3, and the linker pICH41822 were cut/ligated into the level 2 vector pICSL4723 as described. After confirming the constructs, the plasmids were transformed into Agrobacterium strain C58C1. All primers are listed in Supplemental Table S1. The above constructs were introduced into tomato cv Moneyberg by *A. tumefaciens*-mediated transformation (Van Roekel et al., 1993). Homozygous T1 or T2 transgenic plants were used for phenotypic and molecular characterization.

Meristem imaging

Shoot apices were dissected from young plants using a forceps and older leaf primordia were removed to expose

meristems under the stereomicroscope. Immediately after dissection, live meristems were imaged using an euromex scientific camera. To measure meristem size, dissected meristems were imaged under the stereomicroscope (Stemi 508, Zeiss) with a coupled camera (AxioCam IC, Zeiss Germany). Live meristems were imaged immediately after dissection. The SAM size was measured as the maximum width between leaf primordia using Leica Application Suite v4.9 software. CryoSEM images were prepared and imaged at the Wageningen Electron Microscopy Centre on the Magellan 400.

Fruit phenotyping

The second and third inflorescences were used for fruit phenotyping. For each inflorescence, only six flowers were kept and vibrated at anthesis to guarantee successful pollination. Individual fruits were harvested at breaker + 7 (±1 day) for diameter and Brix measurements. Locule number was counted upon fruit cutting for Brix measurements. The Brix measurements were performed in duplo per fruit with an Atago PR-32α digital refractometer.

Meristem transcriptome profiling

The domesticated tomato (*S. lycopersicum*) cultivar Moneyberg and the homozygous *ful1 ful2 mbp10 mbp20* mutant generated in the Moneyberg background were used for transcriptome profiling. For each biological replicate sample, a batch of plants was grown and from each plant, the primary shoot meristem was harvested, either in the VM, TM, or FIM stage. The VM sample contained late VM meristems, just before transition (WT 9-leaf stage; quadruple mutant 12-leaf stage). For the SFIM samples, the first FIM from the sympodial shoot was harvested. About 60 plants were grown per batch (to harvest >30 meristems). All stages were harvested in triplicate for both the WT and quadruple mutant plants. The batches for the different replicates were grown in the greenhouse sequentially. Meristems were dissected using a stereoscope, and tissue was processed for RNA stabilization using an acetone fixation technique (Park et al., 2012). RNA was extracted using the PicoPure RNA Extraction kit (Arcturus). More than 30 meristems were collected for each sample, yielding 1–3-μg RNA, which was enriched for mRNA and processed into cDNA libraries using the Illumina TruSeq Stranded Total RNA LT Sample Prep Kit (Illumina). After quality control (Qubit and Fragment Analyzer), samples were sequenced using Illumina NovaSeq 2 × 150 nt Paired End sequencing. Samples were randomized across sequencing flow cells and lanes within flow cells. After quality control, all data were analyzed using the CLC work package. For data validation, new batches of plants were grown and processed as described above, and the samples were analyzed using RT-qPCR analysis (see Supplemental Table S1 for the primers).

EMSAs

FUL2 and *MBP20* coding sequences were amplified from WT Moneyberg cDNA and cloned into pSPUTK (see Supplemental Table S1 for all primer sequences). The pSPUTK promoter allowed in vitro protein synthesis using the TnT SP6 High-Yield Wheat Germ Protein Expression System (Promega) according to the manufacturer's instructions. The probe fragments consisted of a region of 80–100 bp with the canonical CArG-box in the middle and were amplified from genomic DNA. The mutated probe fragments were generated by overlapping PCR using primers that replaced one base pair in the middle of the CArG-box. EMSAs were performed essentially as described by (Smaczniak et al., 2012b) with minor modifications. Oligonucleotides were fluorescently labelled using DY-682. Labelling was performed by PCR using vector-specific DY-682-labeled primers followed by PCR purification with NucleoSpin Gel and PCR Clean-up kit (MACHEREY-NAGEL). Gel shifts were visualized using a LiCor Odyssey imaging system at 700 nm.

GUS histochemistry

The TCSv2:GUS reporter in the pART27 plasmid was obtained from the Weiss lab (Steiner et al., 2016) and transformed to tomato cultivar Moneyberg as described (Van Roekel et al., 1993). Histochemical analysis of the TCSv2:GUS reporter was performed according to (Soriano et al., 2014). Plant tissue was vacuum infiltrated for 5 min in a solution containing 2.0-mM potassium ferri- and ferrocyanide, and incubated overnight at 37°C. Tissue was then cleared in 70% ethanol prior to imaging.

Accession numbers

FUL1, Solyc06g069430; FUL2, Solyc03g114830; MBP10, Solyc02g065730; MBP20, Solyc02g089210; J, Solyc11g010570; J2, Solyc12g038510; EJ2, Solyc03g114840; TM29, Solyc02g089200; MADS-RIN, Solyc05g012020; TM5, Solyc05g015750; TM3, Solyc01g093965; STM3, Solyc01g092950; SlMBP18, Solyc03g006830; TAG1, Solyc02g071730; SlMBP24, Solyc01g105800; SlMBP13, Solyc08g080100; SlMBP14, Solyc12g056460; SlMBP9, Solyc04g076680; SlMBP12, Solyc12g088090; SlMBP22, Solyc11g005120; MC, Solyc05g056620; AHL15, Solyc12g087950; AP2b, Solyc02g064960; AP2c, Solyc02g093150; AGL6, Solyc01g093960; CKX5, Solyc04g016430; CKX6, Solyc12g008900; CKX8, Solyc10g017990; ARR16, Solyc06g048930. Supplemental Data set S1 contains the accession numbers of the DEGs. The raw data of the RNA-seq experiments has been deposited in GEO under accession number GSE154419

Supplemental data

The following materials are available in the online version of this article.

Supplemental Figure S1. Y2H analysis of FRUITFULL-like proteins with MADS-box proteins from different subfamilies.

Supplemental Figure S2. The truncated FUL1 version is present in many cultivars, but displays the same protein–protein interactions as the full-length reference protein.

Acknowledgments

Funding

References

Aerts N, de Bruijn S, van Mourik H, Angenent GC, van Dijk AD (2018) Comparative analysis of binding patterns of MADS-domain proteins in Arabidopsis thaliana. BMC Plant Biol **18**: 131

Alonge M, Wang X, Benoit M, Soyk S, Pereira L, Zhang L, Suresh H, Ramakrishnan S, Maumus F, Ciren D (2020) Major impacts of widespread structural variation on gene expression and crop improvement in tomato. Cell **182**: 145–161.e23

Balanzà V, Martínez-Fernández I, Sato S, Yanofsky MF, Kaufmann K, Angenent GC, Bemer M, Ferrándiz C (2018) Genetic control of meristem arrest and life span in Arabidopsis by a FRUITFULL-APETALA2 pathway. Nature Commun **9**: 565

Bartrina I, Otto E, Strnad M, Werner T, Schmülling T (2011) Cytokinin regulates the activity of reproductive meristems, flower

organ size, ovule formation, and thus seed yield in Arabidopsis thaliana. Plant Cell **23**: 69–80

Bemer M, Karlova R, Ballester AR, Tikunov YM, Bovy AG, Wolters-Arts M, de Barros Rossetto P, Angenent GC, de Maagd RA (2012) The tomato FRUITFULL homologs TDR4/FUL1 and MBP7/FUL2 regulate ethylene-independent aspects of fruit ripening. Plant Cell **24**: 4437–4451

Bemer M, van Mourik H, Muiño JM, Ferrándiz C, Kaufmann K, Angenent GC (2017) FRUITFULL controls SAUR10 expression and regulates Arabidopsis growth and architecture. J Exp Bot **68**: 3391–3403

Benlloch R, Berbel A, Ali L, Gohari G, Millán T, Madueño F (2015) Genetic control of inflorescence architecture in legumes. Front Plant Sci **6**: 543

Berbel A, Ferrandiz C, Hecht V, Dalmais M, Lund OS, Sussmilch FC, Taylor SA, Bendahmane A, Ellis TN, Beltrán JP (2012) VEGETATIVE1 is essential for development of the compound inflorescence in pea. Nature Commun **3**: 1–8

Bowman JL, Alvarez J, Weigel D, Meyerowitz EM, Smyth DR (1993) Control of flower development in Arabidopsis thaliana by APETALA1 and interacting genes. Development **119**: 721–743

Brownlee BG, Hall RH, Whitty CD (1975) 3-Methyl-2-butenal: an enzymatic degradation product of the cytokinin, N 6-(Δ2-isopentenyl) adenine. Can J Biochem **53**: 37–41

Burko Y, Shleizer-Burko S, Yanai O, Shwartz I, Zelnik ID, Jacob-Hirsch J, Kela I, Eshed-Williams L, Ori N (2013) A role for APETALA1/fruitfull transcription factors in tomato leaf development. Plant Cell **25**: 2070–2083

Chae E, Tan QK-G, Hill TA, Irish VF (2008) An Arabidopsis F-box protein acts as a transcriptional co-factor to regulate floral development. Development **135**: 1235–1245

Cheng X, Li G, Tang Y, Wen J (2018) Dissection of genetic regulation of compound inflorescence development in Medicago truncatula. Development **145**: dev158766

Chuck G, Meeley R, Hake S (2008) Floral meristem initiation and meristem cell fate are regulated by the maize AP2 genes ids1 and sid1. Development **135**: 3013–3019

Consortium TGS, Aflitos S, Schijlen E, de Jong H, de Ridder D, Smit S, Finkers R, Wang J, Zhang G, Li N (2014) Exploring genetic variation in the tomato (Solanum section Lycopersicon) clade by whole-genome sequencing. Plant J **80**: 136–148

D'Agostino IB, Deruere J, Kieber JJ (2000) Characterization of the response of the Arabidopsis response regulator gene family to cytokinin. Plant Physiol **124**: 1706–1717

De Folter S, Immink RG (2011) Yeast protein–protein interaction assays and screens. Methods Mol Biol **754**: 145–165

De Folter S, Immink RG, Kieffer M, Pařenicová L, Henz SR, Weigel D, Busscher M, Kooiker M, Colombo L, Kater MM (2005) Comprehensive interaction map of the Arabidopsis MADS box transcription factors. Plant Cell **17**: 1424–1433

Ferrándiz C, Gu Q, Martienssen R, Yanofsky MF (2000) Redundant regulation of meristem identity and plant architecture by FRUITFULL, APETALA1 and CAULIFLOWER. Development **127**: 725–734

Gao R, Wang Y, Gruber MY, Hannoufa A (2018) miR156/SPL10 modulates lateral root development, branching and leaf morphology in Arabidopsis by silencing AGAMOUS-LIKE 79. Front Plant Sci **8**: 2226

Goslin K, Zheng B, Serrano-Mislata A, Rae L, Ryan PT, Kwaśniewska K, Thomson B, Ó'Maoiléidigh DS, Madueño F, Wellmer F, et al. (2017) Transcription factor interplay between LEAFY and APETALA1/CAULIFLOWER during floral initiation. Plant Physiol **174**: 1097–1109

Gu Q, Ferrándiz C, Yanofsky MF, Martiensson R (1998) The FRUITFULL MADS-box gene mediates cell differentiation during Arabidopsis fruit development. Development **125**: 1509–1517

Han Y, Zhang C, Yang H, Jiao Y (2014) Cytokinin pathway mediates APETALA1 function in the establishment of determinate floral meristems in Arabidopsis. Proc Natl Acad Sci USA **111**: 6840–6845

Immink RG, Tonaco IA, de Folter S, Shchennikova A, van Dijk AD, Busscher-Lange J, Borst JW, Angenent GC (2009) SEPALLATA3: the 'glue' for MADS box transcription factor complex formation. Genome Biol 10: R24

Jaakola L, Poole M, Jones MO, Kämäräinen-Karppinen T, Koskimäki JJ, Hohtola A, Häggman H, Fraser PD, Manning K, King GJ (2010) A SQUAMOSA MADS box gene involved in the regulation of anthocyanin accumulation in bilberry fruits. Plant Physiol 153: 1619–1629

Jaudal M, Zhang L, Che C, Putterill J (2015) Three Medicago MtFUL genes have distinct and overlapping expression patterns during vegetative and reproductive development and 35S: MtFULb accelerates flowering and causes a terminal flower phenotype in Arabidopsis. Front Genet 6: 50

Jia Z, Jiang B, Gao X, Yue Y, Fei Z, Sun H, Wu C, Sun S, Hou W, Han T (2015) GmFULa, a FRUITFULL homolog, functions in the flowering and maturation of soybean. Plant Cell Rep 34: 121–132

Jung JH, Lee HJ, Ryu JY, Park CM (2016) SP L3/4/5 Integrate Developmental Aging and Photoperiodic Signals into the FT-FD Module in Arabidopsis Flowering. Mol Plant 9: 1647–1659

Karami O, Rahimi A, Khan M, Bemer M, Hazarika RR, Mak P, Compier M, van Noort V, Offringa R (2020) A suppressor of axillary meristem maturation promotes longevity in flowering plants. bioRxiv. doi: 10.1101/2020.01.03.893875

Kardailsky I, Shukla VK, Ahn JH, Dagenais N, Christensen SK, Nguyen JT, Chory J, Harrison MJ, Weigel D (1999) Activation tagging of the floral inducer FT. Science 286: 1962–1965

Karlova R, Rosin FM, Busscher-Lange J, Parapunova V, Do PT, Fernie AR, Fraser PD, Baxter C, Angenent GC, de Maagd RA (2011) Transcriptome and metabolite profiling show that APETALA2a is a major regulator of tomato fruit ripening. Plant Cell 23: 923–941

Kaufmann K, Muino JM, Jauregui R, Airoldi CA, Smaczniak C, Krajewski P, Angenent GC (2009) Target genes of the MADS transcription factor SEPALLATA3: integration of developmental and hormonal pathways in the Arabidopsis flower. PLoS Biol 7: e1000090

Kaufmann K, Wellmer F, Muiño JM, Ferrier T, Wuest SE, Kumar V, Serrano-Mislata A, Madueno F, Krajewski P, Meyerowitz EM (2010) Orchestration of floral initiation by APETALA1. Science 328: 85–89

Kurakawa T, Ueda N, Maekawa M, Kobayashi K, Kojima M, Nagato Y, Sakakibara H, Kyozuka J (2007) Direct control of shoot meristem activity by a cytokinin-activating enzyme. Nature 445: 652–655

Lee J, Lee I (2010) Regulation and function of SOC1, a flowering pathway integrator. J Exp Bot 61: 2247–2254

Leseberg CH, Eissler CL, Wang X, Johns MA, Duvall MR, Mao L (2008) Interaction study of MADS-domain proteins in tomato. J Exp Bot 59: 2253–2265

Levy YY, Mesnage S, Mylne JS, Gendall AR, Dean C (2002) Multiple roles of Arabidopsis VRN1 in vernalization and flowering time control. Science 297: 243–246

Li C, Lin H, Chen A, Lau M, Jernstedt J, Dubcovsky J (2019) Wheat VRN1 and FUL2 play critical and redundant roles in spikelet meristem identity and spike determinacy. bioRxiv: 510388

Lifschitz E, Eviatar T, Rozman A, Shalit A, Goldshmidt A, Amsellem Z, Alvarez JP, Eshed Y (2006) The tomato FT ortholog triggers systemic signals that regulate growth and flowering and substitute for diverse environmental stimuli. Proc Natl Acad Sci USA 103: 6398–6403

Lippman ZB, Cohen O, Alvarez JP, Abu-Abied M, Pekker I, Paran I, Eshed Y, Zamir D (2008) The making of a compound inflorescence in tomato and related nightshades. PLoS Biol 6: e288

Litt A, Irish VF (2003) Duplication and diversification in the APETALA1/FRUITFULL floral homeotic gene lineage: implications for the evolution of floral development. Genetics 165: 821–833

Liu C, Teo ZWN, Bi Y, Song S, Xi W, Yang X, Yin Z, Yu H (2013) A conserved genetic pathway determines inflorescence architecture in Arabidopsis and rice. Dev Cell 24: 612–622

Liu D, Wang D, Qin Z, Zhang D, Yin L, Wu L, Colasanti J, Li A, Mao L (2014) The SEPALLATA MADS-box protein SLMBP 21 forms protein complexes with JOINTLESS and MACROCALYX as a transcription activator for development of the tomato flower abscission zone. Plant J 77: 284–296

MacAlister CA, Park SJ, Jiang K, Marcel F, Bendahmane A, Izkovich Y, Eshed Y, Lippman ZB (2012) Synchronization of the flowering transition by the tomato TERMINATING FLOWER gene. Nat Genet 44: 1393

Maheepala DC, Emerling CA, Rajewski A, Macon J, Strahl M, Pabón-Mora N, Litt A (2019) Evolution and diversification of FRUITFULL genes in Solanaceae. Front Plant Sci 10: 43

Mandel MA, Gustafson-Brown C, Savidge B, Yanofsky MF (1992) Molecular characterization of the Arabidopsis floral homeotic gene APETALA1. Nature 360: 273–277

Matsuo S, Kikuchi K, Fukuda M, Honda I, Imanishi S (2012) Roles and regulation of cytokinins in tomato fruit development. J Exp Bot 63: 5569–5579

McCarthy EW, Mohamed A, Litt A (2015) Functional divergence of APETALA1 and FRUITFULL is due to changes in both regulation and coding sequence. Front Plant Sci 6: 1076

McGarry RC, Ayre BG (2012) Manipulating plant architecture with members of the CETS gene family. Plant Sci 188–189: 71–81

McGaw BA, Horgan R (1983) Cytokinin catabolism and cytokinin oxidase. Phytochemistry 22: 1103–1105

Melzer S, Lens F, Gennen J, Vanneste S, Rohde A, Beeckman T (2008) Flowering-time genes modulate meristem determinacy and growth form in Arabidopsis thaliana. Nat Genet 40: 1489

Molinero-Rosales N, Latorre A, Jamilena M, Lozano R (2004) SINGLE FLOWER TRUSS regulates the transition and maintenance of flowering in tomato. Planta 218: 427–434

Molinero-Rosales N, Jamilena M, Zurita S, Gómez P, Capel J, Lozano R (1999) FALSIFLORA, the tomato orthologue of FLORICAULA and LEAFY, controls flowering time and floral meristem identity. Plant J 20: 685–693

Morel P, Chambrier P, Boltz V, Chamot S, Rozier F, Bento SR, Trehin C, Monniaux M, Zethof J, Vandenbussche M (2019) Divergent functional diversification patterns in the SEP/AGL6/AP1 MADS-box transcription factor superclade. Plant Cell 31: 3033–3056

Morel P, Heijmans K, Rozier F, Zethof J, Chamot S, Bento SR, Vialette-Guiraud A, Chambrier P, Trehin C, Vandenbussche M (2017) Divergence of the floral A-function between an asterid and a rosid species. Plant Cell 29: 1605–1621

Nakano T, Kimbara J, Fujisawa M, Kitagawa M, Ihashi N, Maeda H, Kasumi T, Ito Y (2012) MACROCALYX and JOINTLESS interact in the transcriptional regulation of tomato fruit abscission zone development. Plant Physiol 158: 439–450

Pabón-Mora N, Ambrose BA, Litt A (2012) Poppy APETALA1/FRUITFULL orthologs control flowering time, branching, perianth identity, and fruit development. Plant Physiol 158: 1685–1704

Pabón-Mora N, Sharma B, Holappa LD, Kramer EM, Litt A (2013) The Aquilegia FRUITFULL-like genes play key roles in leaf morphogenesis and inflorescence development. Plant J 74: 197–212

Park SJ, Jiang K, Schatz MC, Lippman ZB (2012) Rate of meristem maturation determines inflorescence architecture in tomato. Proc Natl Acad Sci USA 109: 639–644

Périlleux C, Bouché F, Randoux M, Orman-Ligeza B (2019) Turning meristems into fortresses. Trends Plant Sci 24: 431–442

Ping J, Liu Y, Sun L, Zhao M, Li Y, She M, Sui Y, Lin F, Liu X, Tang Z (2014) Dt2 is a gain-of-function MADS-domain factor gene that specifies semideterminacy in soybean. Plant Cell 26: 2831–2842

Pnueli L, Carmel-Goren L, Hareven D, Gutfinger T, Alvarez J, Ganal M, Zamir D, Lifschitz E (1998) The SELF-PRUNING gene of tomato regulates vegetative to reproductive switching of sympodial meristems and is the ortholog of CEN and TFL1. Development **125**: 1979–1989

Porebski S, Bailey LG, Baum BR (1997) Modification of a CTAB DNA extraction protocol for plants containing high polysaccharide and polyphenol components. Plant Mol Biol Rep **15**: 8–15

Roldan MVG, Périlleux C, Morin H, Huerga-Fernandez S, Latrasse D, Benhamed M, Bendahmane A (2017) Natural and induced loss of function mutations in SlMBP21 MADS-box gene led to jointless-2 phenotype in tomato. Sci Rep **7**: 4402

Roohanitaziani R, de Maagd RA, Lammers M, Molthoff J, Meijer-Dekens F, van Kaauwen MPW, Finkers R, Tikunov Y, Visser RGF, Bovy AG (2020) Exploration of a resequenced tomato core collection for phenotypic and genotypic variation in plant growth and fruit quality traits. Genes **11**: 1278

Sablowski R (2007) Flowering and determinacy in Arabidopsis. J Exp Bot **58**: 899–907

Serrano-Mislata A, Goslin K, Zheng B, Rae L, Wellmer F, Graciet E, Madueño F (2017) Regulatory interplay between LEAFY, APETALA1/CAULIFLOWER and TERMINAL FLOWER1: new insights into an old relationship. Plant Signal Behav **12**: e1370164–e1370164

Shalit-Kaneh A, Eviatar-Ribak T, Horev G, Suss N, Aloni R, Eshed Y, Lifschitz E (2019) The flowering hormone florigen accelerates secondary cell wall biogenesis to harmonize vascular maturation with reproductive development. Proc Natl Acad Sci USA **116**: 16127–16136

Shima Y, Kitagawa M, Fujisawa M, Nakano T, Kato H, Kimbara J, Kasumi T, Ito Y (2013) Tomato FRUITFULL homologues act in fruit ripening via forming MADS-box transcription factor complexes with RIN. Plant Mol Biol **82**: 427–438

Smaczniak C, Immink RG, Angenent GC, Kaufmann K (2012a) Developmental and evolutionary diversity of plant MADS-domain factors: insights from recent studies. Development **139**: 3081–3098

Smaczniak C, Immink RG, Muiño JM, Blanvillain R, Busscher M, Busscher-Lange J, Dinh QP, Liu S, Westphal AH, Boeren S (2012b) Characterization of MADS-domain transcription factor complexes in Arabidopsis flower development. Proc Natl Acad Sci USA **109**: 1560–1565

Soriano M, Li H, Jacquard C, Angenent GC, Krochko J, Offringa R, Boutilier K (2014) Plasticity in cell division patterns and auxin transport dependency during in vitro embryogenesis in Brassica napus. The Plant Cell **26**: 2568–2581

Souer E, Rebocho AB, Bliek M, Kusters E, de Bruin RA, Koes R (2008) Patterning of inflorescences and flowers by the F-Box protein DOUBLE TOP and the LEAFY homolog ABERRANT LEAF AND FLOWER of petunia. Plant Cell **20**: 2033–2048

Soyk S, Lemmon ZH, Oved M, Fisher J, Liberatore KL, Park SJ, Goren A, Jiang K, Ramos A, van der Knaap E (2017) Bypassing negative epistasis on yield in tomato imposed by a domestication gene. Cell **169**: 1142–1155.e12

Soyk S, Lemmon ZH, Sedlazeck FJ, Jiménez-Gómez JM, Alonge M, Hutton SF, Van Eck J, Schatz MC, Lippman ZB (2019) Duplication of a domestication locus neutralized a cryptic variant that caused a breeding barrier in tomato. Nat Plants **5**: 471

Steiner E, Israeli A, Gupta R, Shwartz I, Nir I, Leibman-Markus M, Tal L, Farber M, Amsalem Z, Ori N (2020) Characterization of the cytokinin sensor TCSv2 in arabidopsis and tomato. Plant Methods **16**: 1–12

Steiner E, Livne S, Kobinson-Katz T, Tal L, Pri-Tal O, Mosquna A, Tarkowská De, Mueller B, Tarkowski P, Weiss D (2016) The putative *O*-linked *N*-acetylglucosamine transferase SPINDLY inhibits class I TCP proteolysis to promote sensitivity to cytokinin. Plant Physiol **171**: 1485–1494

Szymkowiak EJ, Irish EE (2006) JOINTLESS suppresses sympodial identity in inflorescence meristems of tomato. Planta **223**: 646–658

Theissen G, Saedler H (2001) Floral quartets. Nature **409**: 469–471

Thouet J, Quinet M, Lutts S, Kinet J-M, Périlleux C (2012) Repression of floral meristem fate is crucial in shaping tomato inflorescence. PLoS ONE **7**

Thouet J, Quinet M, Ormenese S, Kinet J-M, Périlleux C (2008) Revisiting the involvement of SELF-PRUNING in the sympodial growth of tomato. Plant Physiol **148**: 61–64

Van Dijk AD, Morabito G, Fiers M, van Ham RC, Angenent GC, Immink RG (2010) Sequence motifs in MADS transcription factors responsible for specificity and diversification of protein-protein interaction. PLoS Comput Biol **6**: e1001017

Van Roekel JS, Damm B, Melchers LS, Hoekema A (1993) Factors influencing transformation frequency of tomato (*Lycopersicon esculentum*). Plant Cell Rep **12**: 644–647

Wang R, da Rocha Tavano EC, Lammers M, Martinelli AP, Angenent GC, de Maagd RA (2019) Re-evaluation of transcription factor function in tomato fruit development and ripening with CRISPR/Cas9-mutagenesis. Sci Rep **9**: 1696

Wang S, Lu G, Hou Z, Luo Z, Wang T, Li H, Zhang J, Ye Z (2014a) Members of the tomato FRUITFULL MADS-box family regulate style abscission and fruit ripening. J Exp Bot **65**: 3005–3014

Wang Y, Wang J, Shi B, Yu T, Qi J, Meyerowitz EM, Jiao Y (2014b) The stem cell niche in leaf axils is established by auxin and cytokinin in Arabidopsis. Plant Cell **26**: 2055–2067

Wang J-W, Czech B, Weigel D (2009) miR156-regulated SP L transcription factors define an endogenous flowering pathway in Arabidopsis thaliana. Cell **138**: 738–749

Weber E, Gruetzner R, Werner S, Engler C, Marillonnet S (2011) Assembly of designer TAL effectors by Golden Gate cloning. PLoS ONE **6**: e19722

Werner T, Motyka V, Laucou V, Smets R, Van Onckelen H, Schmülling T (2003) Cytokinin-deficient transgenic Arabidopsis plants show multiple developmental alterations indicating opposite functions of cytokinins in the regulation of shoot and root meristem activity. Plant Cell **15**: 2532–2550

Würschum T, Gross-Hardt R, Laux T (2006) APETALA2 regulates the stem cell niche in the Arabidopsis shoot meristem. Plant Cell **18**: 295–307

Yant L, Mathieu J, Dinh TT, Ott F, Lanz C, Wollmann H, Chen X, Schmid M (2010) Orchestration of the floral transition and floral development in Arabidopsis by the bifunctional transcription factor APETALA2. Plant Cell **22**: 2156–2170

Ye L, Wang B, Zhang W, Shan H, Kong H (2016) Gains and losses of cis-regulatory elements led to divergence of the Arabidopsis APETALA1 and CAULIFLOWER duplicate genes in the time, space, and level of expression and regulation of one paralog by the other. Plant Physiol **171**: 1055–1069

Yuste-Lisbona FJ, Quinet M, Fernández-Lozano A, Pineda B, Moreno V, Angosto T, Lozano R (2016) Characterization of vegetative inflorescence (mc-vin) mutant provides new insight into the role of MACROCALYX in regulating inflorescence development of tomato. Sci Rep **6**: 18796

Zhang P, Wang R, Wang X, Mysore KS, Wen J, Meng Y, Gu X, Niu L, Lin H (2021) MtFULc controls inflorescence development by directly repressing MtTFL1 in Medicago truncatula. J Plant Physiol **256**: 153329

Zhao J, Jiang L, Che G, Pan Y, Li Y, Hou Y, Zhao W, Zhong Y, Ding L, Yan S (2019) A functional allele of CsFUL1 regulates fruit length through repressing CsSUP and inhibiting auxin transport in cucumber. Plant Cell **31**: 1289–1307

Zhu Y, Klasfeld S, Jeong CW, Jin R, Goto K, Yamaguchi N, Wagner D (2020) TERMINAL FLOWER 1-FD complex target genes and competition with FLOWERING LOCUS T. Nat Commun **11**: 5118